

In-Space Propulsion Engine Architecture Based on Sublimation of Planetary Resources: From Exploration Robots to NEO Mitigation

**2011 – 2012
Final Report**

To

NASA Innovative Advanced Concepts

Laurent Sibille
Engineering Services Contract, Kennedy Space Center, Florida

James G. Mantovani
NASA, Surface Systems Office, NE-S, Kennedy Space Center, Florida

Jesus A. Dominguez
Engineering Services Contract, Kennedy Space Center, Florida

CONTENTS

| | |
|--|----|
| 1. INTRODUCTION | 1 |
| 2. ICES IN THE SOLAR SYSTEM: A UBIQUITOUS AND VAST RESOURCE | 1 |
| 3. ENERGY CONVERSION SCHEMES USING PLANETARY RESOURCES | 2 |
| 4. ORBITAL CHANGE OF NEAR-EARTH OBJECT BY <i>IN SITU</i> PROPULSION | 3 |
| 5. FEASIBILITY: ENERGY REQUIREMENTS FOR ICE UTILIZATION..... | 4 |
| 5.1 Sublimation of Ice in the Solar System..... | 4 |
| 5.2 Volatilization of Mineral Oxides | 10 |
| 5.3 Excavation and Collection of Ice Resources | 12 |
| 6. FEASIBILITY: POWER OUTPUTS FROM SUBLIMATED ICE GASES | 16 |
| 6.1 Propulsion 16 | |
| 6.1.1 Thrust Model..... | 17 |
| 6.2 Pneumatics 20 | |
| 6.2.1 Pneumatic Transport of Solids Using Martian CO ₂ | 21 |
| 6.2.2 Solid-Gas Flow Model: Fundamentals | 22 |
| 6.2.3 Model Validation on Eductor Operation..... | 24 |
| 6.2.4 Experimental Setup to Validate Model on Eductor Performance..... | 25 |
| 6.2.5 Model Validation Using Experimental Data..... | 26 |
| 6.3 Energy Sources for Conversion Applications..... | 27 |
| 7. APPLICATION CONCEPTS OF IN-SPACE PROPULSION USING PLANETARY RESOURCES | 28 |
| 7.1 Cold/Warm Gas Propulsion for Hoppers..... | 28 |
| 7.2 Compressed Gas Launch of Ballistic Objects..... | 35 |
| 7.3 Hovercraft (Surface Sublimation of Ice Sheets) | 36 |
| 7.4 Pneumatic Regolith Transfer Using Low Pressure CO ₂ | 37 |
| 8. SPECIAL APPLICATION: ASTEROID AND COMET DEFLECTION BY EJECTION OF <i>IN SITU</i> VOLATILES | 40 |
| 9. CONCLUSION..... | 43 |
| 10. ACKNOWLEDGEMENTS..... | 44 |
| 11. REFERENCES | 44 |
| Appendix A. PHASE CONDITIONS OF WATER IN THE SOLAR SYSTEM | 1 |
| Appendix B. PHASE CONDITIONS OF CO ₂ IN THE SOLAR SYSTEM..... | 8 |
| Appendix C. PHASE CONDITIONS OF CH ₄ IN THE SOLAR SYSTEM..... | 14 |

FIGURES

| | | |
|------------|---|----|
| Table 1. | Molecules detected as ices on outer solar system planets and satellites* | 4 |
| Figure 1. | Phase diagram of water with conditions existing in the Solar System..... | 5 |
| Figure 2. | Phase diagram of CO ₂ with conditions existing in the Solar System..... | 6 |
| Figure 3. | Enthalpy of sublimation of H ₂ O at 7.5 x 10 ⁻⁹ torr: (a) Calculated using HSC Chemistry and (b) reported from Feistel et al., 2007 | 8 |
| Figure 4. | Enthalpy of sublimation of water ice mixed with regolith..... | 8 |
| Figure 5. | Evolution of gaseous specie from a pool of molten regolith under vacuum conditions (10 ⁻⁷ torr) | 11 |
| Figure 6. | Thermal spalling (left) involves thermally fracturing a rock formation. Thermal selting (right) involves the melting and evaporation of a rock formation..... | 13 |
| Figure 7. | Operational steps in the plunge method for pneumatically excavating and lifting regolith | 15 |
| Figure 8. | Notional deployable cover for enhancing surface optical properties as well as providing a collection volume for collecting cold steam. (Mungas, 2006)..... | 16 |
| Figure 9. | Comparison of common propulsion systems based on actual system mass and total impulse generated (Brown, 1996)..... | 17 |
| Figure 10. | 3D spatial domain used in the thruster model to compute thrust performance of carbon dioxide, methane, and water steam..... | 18 |
| Figure 11. | 2D domain (a) and gas flow location points (b) used in the simplified transient thrust model..... | 18 |
| Figure 12. | Assembly and connectivity of the operation units used to pneumatically transport Martian material using CO ₂ gas..... | 21 |
| Figure 13. | Eductor BCs used in the model based on actual experimental setting..... | 24 |
| Figure 14. | Particle velocity profile forecasted by the model using the BCs of Figure 13..... | 25 |
| Figure 15. | Experimental setup to validate model on the eductor performance | 26 |
| Figure 16. | Experimental validation of the eductor performance model | 26 |
| Figure 17. | Small robotic exploration spacecraft collect and sublimate CO ₂ ice at the Martian polar cap to use in attitude-control thrusters | 28 |
| Figure 18. | Critical PT (Pressure-Temperature) coordinates and molecular weight of water, CO ₂ , CH ₄ , O ₂ , CO, and N ₂ | 29 |
| Figure 19. | Modeled path conditions inside the tank originally filled with superheated water vapor at 2,900 psi and 923 K to generate thrust..... | 30 |
| Figure 20. | Modeled transient thrust and temperature profiles (at the tank throat and the nozzle) when tank is initially filled with water vapor at 2,900 psi and 923 K to generate thrust..... | 31 |
| Figure 21. | Modeled path conditions inside the tank originally filled with CO ₂ gas at 2,900 psi and 513 K to generate thrust | 32 |
| Figure 22. | Modeled transient thrust and temperature (at the throat and the nozzle) profiles as the tank is originally filled with CO ₂ gas at 2,900 psi and 513 K to generate thrust..... | 33 |

| | | |
|------------|--|----|
| Figure 23. | Modeled path conditions inside the tank originally filled with CH ₄ gas at 2,900 psi and 700 K to generate thrust | 34 |
| Figure 24. | Modeled transient thrust and temperature (at the throat and the nozzle) profiles as the tank is originally filled with CH ₄ gas at 2,900 psi and 700 K to generate thrust..... | 35 |
| Figure 25. | Small payloads ballistic trajectories in lunar gravity using CO ₂ as cold gas propellant with initial tank conditions: 300 bar, 513 K, gas mass 3.2 kg. Launch angle is 60° | 36 |
| Figure 26. | CO ₂ gas velocity profile modeled using two nozzles with the area equal to the total area of small nozzles actually in place inside the hopper | 38 |
| Figure 27. | Transient particle (solid phase) velocity profile modeled using the gas flow conditions of Figure 24 | 39 |
| Figure 28. | Solid mass flow rates predicted for various eductor/hopper pressures to convey regolith at different heights | 40 |
| Figure 29. | Ejected mass flow rate from a comet or asteroid to propel it on a deflected orbit with a Δv of 0.1m/s..... | 41 |
| Figure 30. | Conceptual mission to deflect a comet by using <i>in situ</i> propulsion | 43 |
| Figure 31. | Water phase equilibrium at moderate pressure [1]..... | 1 |
| Figure 32. | Water solid-vapor phase equilibrium (including vacuum conditions) measured by various researchers [2]..... | 2 |
| Figure 33. | Daytime and nighttime temperature observations of the lunar south pole recorded by the Diviner Radiometer Experiment, one of seven instruments on NASA’s Lunar Reconnaissance Orbiter | 2 |
| Figure 34. | Ambient conditions on the Moon (colored in pink) that support the presence of water ice on the lunar surface | 3 |
| Figure 35. | Mars surface temperature profile measured at night by the Thermal Emission Spectrometer (TES) onboard the Mars Global Surveyor spacecraft | 3 |
| Figure 36. | Ambient conditions on Mars (marked with dashed red line) that would support the presence of water ice on the Mars surface | 4 |
| Figure 37. | Ambient conditions on a comet (marked with dashed red line) that would support the presence of water ice on the comet’s surface..... | 5 |
| Figure 38. | Ambient conditions on Europa (marked with dashed red line) that would support the presence of water ice on Europa’s surface..... | 6 |
| Figure 39. | Ambient conditions on Titan (marked with dashed red line) that would support the presence of water ice on Titan’s surface..... | 7 |
| Figure 40. | CO ₂ solid-gas phase equilibrium estimated and reported independently by several authors [1]..... | 8 |
| Figure 41. | Ambient conditions on the Moon (colored in blue) that support the presence of CO ₂ ice on the lunar surface | 9 |
| Figure 42. | Mars surface temperature profile measured at night by TES onboard the Mars Global Surveyor spacecraft..... | 10 |
| Figure 43. | Ambient conditions on Mars (marked with continuous red line) that would support the presence of CO ₂ ice on the Mars surface | 10 |
| Figure 44. | Ambient conditions on a comet (marked with continuous red line) that would support the presence of CO ₂ ice on the comet’s surface..... | 12 |

| | | |
|------------|---|----|
| Figure 45. | Ambient conditions on Europa (marked with continuous red line) that would support the presence of CO ₂ ice on Europa's surface..... | 12 |
| Figure 46. | Ambient conditions on Titan (marked with continuous red line) that would support the presence of CO ₂ ice on Titan's surface | 13 |
| Figure 47. | CH ₄ sublimation equilibrium measurement and estimation of Antoine parameters (A, B, & C) independently obtained by four authors within the temperature range of 91-190 K [1]. This liquid-gas saturation line is extrapolated (dashed line) to predict sublimation line at lower temperature and pressure | 15 |
| Figure 48. | Daytime and nighttime temperature observations of the lunar south pole recorded by the Diviner Radiometer Experiment, one of seven instruments on NASA's Lunar Reconnaissance Orbiter | 16 |
| Figure 49. | CH ₄ ice is not likely to be present on the lunar surface because the Moon's lowest surface temperature of 40 K is higher than 25 K, the highest temperature at which CH ₄ ice exists at the Moon's ambient pressure range (E-10 to E-14 torr)..... | 16 |
| Figure 50. | Mars surface temperature profile measured at night by TES onboard the Mars Global Surveyor spacecraft..... | 17 |
| Figure 51. | CH ₄ ice is not likely to be present on the Mars surface because the lowest Mars surface temperature is 125 K and CH ₄ vapor pressure at 125 K is 2,000 torr, much higher than the Mars ambient pressure (5 torr) | 17 |
| Figure 52. | CH ₄ ice is not likely to be present on a comet's surface because the lowest comet surface temperature 40 K is higher than 22 K, the highest temperature at which CH ₄ ice exists at the comet's ambient pressure (E-14 torr) | 18 |
| Figure 53. | Ambient conditions on Europa (marked with continuous red line) that would support the presence of CH ₄ ice on Europa's surface..... | 19 |
| Figure 54. | Ambient conditions on Titan (marked with continuous red line) that would support the presence of liquid CH ₄ on Titan's surface | 20 |

TABLES

| | | |
|----------|--|---|
| Table 1. | Molecules detected as ices on outer solar system planets and satellites* | 4 |
|----------|--|---|

ABSTRACT

Volatile solids occur naturally on most planetary bodies, including the Moon, Mars, asteroids, and comets. Carbon dioxide and water ices have been detected remotely at the poles or in permanently shadowed craters on Mars and on the Moon. Comets consist mostly of ice (>85% of mass), and some asteroids also contain solid ices in various amounts. In the outer Solar System, moons of the giant planets host the same resources; Ganymede, Europa, and Callisto are composed of silicate rock and water ice to varying degrees, and the Cassini-Huygens probe has revealed methane snow and water ice crusts on Titan.

We investigate the concept of sublimating these ices and minerals to form gases where favorable environmental conditions prevail on many bodies in the Solar System. The applications offered by this resource sublimation concept range from powering surface systems during planetary missions to using in-space propulsion to deflect near-Earth objects (NEOs) threatening our planet.

1. INTRODUCTION

To date, the use of solar radiation to provide onboard electrical power remains the sole application of a space resource that has been exploited to sustain exploration missions. Even if one includes vacuum and the thermal sink offered by interplanetary space as exploited resources, our fleet of spacecraft is designed to operate in space without tapping the vast potential of this environment. We propose to break through the paradigm and demonstrate the feasibility of a novel architecture concept based on the extensive use of volatile space resources to generate propulsive and mechanical power for a variety of space missions. The concept also departs from other *in situ* resource utilization (ISRU) schemes by its inherent simplicity in applying heat to cause a change of state rather than to induce a chemical reaction. Furthermore, we explore the possible application of the concept to propel large near-Earth objects (NEOs) off their course and address a critical issue confronting us in the coming decades—how to protect Earth from the threat of an impact by an asteroid or comet.

The paradigm shift in space exploration created by the use of space resources extends beyond ensuring the survival of human crews. It is transformative also in its ability to offer *in situ* solutions to the need for power generation and to mitigate spaceborne threats. We explore here a potentially widely applicable concept of using low ambient pressures and heating various compounds to generate propulsive power or to actuate mechanisms through the release of formed gases. The concept opens possibilities for missions to planetary surfaces because it accesses a local resource that greatly extends the mobility of crews and robotics and increases the capability for power generation. Both of these challenges are among the greatest to be faced in missions to remote worlds. The confirmed presence of volatile solids such as carbon dioxide (CO₂) and water ice on the Moon, Mars, asteroids, and comets makes these resources good candidates for use in mission architecture. The concept is also being studied to include compounds such as methane (CH₄), and other hydrocarbons that are thought to exist in solid form on some of the planetoids and moons in the outer Solar System (e.g., Europa and Titan). The need to rely upon a single form of energy for all surface activities remains a concern for exploration missions. Radioisotope thermoelectric generators (RTGs) and their successors are now very reliable over many years (as demonstrated by the Voyager spacecraft), but they power only electrical systems, as do solar photovoltaics. We propose to revolutionize the capability of planetary surface missions by complementing the all-electrical approach by using gas heating and compression to convert the potential energy in volatile space resources into propulsive thrust and mechanical force.

2. ICES IN THE SOLAR SYSTEM: A UBIQUITOUS AND VAST RESOURCE

Surveys of the planetary environmental conditions and the states of matter for major compounds (water, CO₂, and CH₄) are provided in the appendices. These compounds are found in quantities ranging from a few tons (on asteroids in the Jovian rings) to billions of tons (on planets and moons with remarkably diverse landscape features and deposits). Each destination offers unique characteristics that present different design and operational challenges in acquiring those resources. The various applications also lead to

a wide range of opportunities for applications in spacecraft systems, several of which are treated in this preliminary study.

3. ENERGY CONVERSION SCHEMES USING PLANETARY RESOURCES

All space endeavors require power, and their success depends on the ability to balance the supply of energy to systems that must operate concurrently. As space missions venture farther and farther beyond Earth's orbital space, longer mission times require power systems with higher reliability, but the choices become more limited. Missions operating on planetary surfaces have needs such as powering mobility systems and communication devices, operating thermal control systems, and performing a variety of other tasks. Exploration tasks include collecting and transporting material, drilling and excavation, and powering and controlling scientific instrumentation. All planetary exploration missions continue to rely on electrical energy as the sole source of power. Photovoltaic solar panels have been typically used for missions within the orbit of Mars (inner solar system), and RTGs must be used in the outer solar system. The decision to power the Mars Science Laboratory with an RTG is a departure from the use of solar photovoltaics on Mars rovers; it allows for more potential landing locations, including those where solar illumination is less, and it makes more power available to the larger craft. It also offers greater thermal control by providing the spacecraft systems with power from the heat generated by radioactive decay.

In the past two decades, science missions to the Moon, Mars, several asteroids, and the moons of Jupiter and Saturn have gathered strong evidence for the presence of water ice in the Solar System (Dalton, 2010; Colaprete, 2010; Showman, 1999). Harvesting this resource could revolutionize space exploration. The recent Lunar Reconnaissance Orbiter (LRO)/Lunar LCROSS mission put an exclamation point on a decade-long suite of international missions by providing remote-sensing maps of lunar water ice at polar latitudes and direct detection of such ice that resulted from an impact into Cabeus crater. According to Colaprete, et al., "the water contained in just [the] Cabeus crater would be enough to launch the Space Shuttle 2000 times" if hydrogen/oxygen cryogenic liquid propellants could be produced *in situ* from it (Colaprete, 2010). On Mars, orbiting remote sensing platforms (Odyssey and Mars Global Surveyor) have repeatedly detected (Demidov, 2011) a hydrogen signature presumed to come from subsurface permafrost ice deposits. Moreover, the Phoenix Mars Lander mission established convincingly that water ice is present in the subsurface near the Martian north pole (Arvidson, 2009). Beyond Mars, asteroids, such as the dwarf planet Ceres, are thought to contain an icy mantle above a rocky core (Rivkin, 2010). In 2010, the EPOXI mission spacecraft revealed a cometary snowstorm around comet Hartley 2, created by carbon dioxide jets spewing out tons of golf-ball-to-basketball-sized fluffy ice particles from the peanut-shaped comet's rocky ends. At the same time, a different process was causing water vapor to escape from the comet's smooth midsection. The Galileo mission to the Jovian system and the Cassini-Huygens mission to Saturn and its moons have added a wealth of knowledge to the Voyager data in the past decade. Around Jupiter, Ganymede, and Callisto appear to be composed of approximately equal amounts of silicate rocks and water ice. Callisto has also revealed the presence of carbon dioxide and organic

compounds (Kuskov, 2005; Showman, 1999). Europa's surface contains much water ice under a tenuous atmosphere of oxygen. In 2004–2005, the Saturnian moon Titan was explored by the Huygens landing probe, unveiling an extraordinary world of hydrocarbon seas (CH₄ and ethane) on a body of silicate rocks and water ice, with CH₄ snow. The atmosphere of Titan is denser than that of Earth, with a surface pressure about 1.45 times that of Earth's (Coustenis, 2008). Because the atmosphere is so thick and the gravity so low (0.14 G), flight is possible on Titan (Zubrin, 1999). After landing, Huygens photographed a dark plain composed of water ice covered in small rocks and pebbles (ESA News, 2005).

This abundance of data makes these solid volatile resources good candidates for use in the proposed mission architecture concept. In low-pressure environments, direct sublimation of ices in propulsion chambers could provide mobility for roving or hovering and for actuating pneumatic systems to lift, transport, and operate machinery. The RTG provides an obvious heat source for efficient conversion of these solids into gases at the right temperatures. Solar collection systems can also provide this in the same way, and other heat systems (laser, resistive heaters) can be powered electrically as well. This new energy architecture is then complementary and acts as a multiplier for existing energy sources. Using local consumables to power systems will change the paradigm of the mission architecture and increase safety factors and capabilities. It also changes the economic equation that controls the cost of the scientific exploration of planets; the large investment in time and direct costs makes it imperative to achieve mission goals because a follow-up mission may not be scheduled for a long time. A new power source such as "sublimation pneumatics" would improve the chances of accomplishing or extending mission objectives. The same logic applies to human exploration of planetary surfaces to an even greater extent because the new power source empowers those best able to respond to changing situations. On worlds with a thick atmosphere and very low gravity, such as Titan, the sublimation of volatile solids could power steam propeller engines. In contrast, sublimation rocket engines would find application to propel surface and flying vehicles in low gravity in the near-vacuum atmosphere of Europa.

4. ORBITAL CHANGE OF NEAR-EARTH OBJECT BY *IN SITU* PROPULSION

The concept of sublimation pneumatics is extended to a larger scale by considering whether the sublimation of volatile solids (CO₂, water) and the volatilization of mineral compounds found in asteroids and comets can provide the propulsive force needed to alter the orbits of near-Earth objects in order to avoid a catastrophic collision with Earth.

By definition, NEOs are objects whose closest approach to the Sun (perihelion) is less than 1.3 AU units. Potentially hazardous objects (PHOs) are objects that pass within 0.05 AU of Earth (7.5 million km) and can penetrate Earth's atmosphere. Although an accurate threat assessment requires knowledge of the characteristics of the object, the current view is that a stony asteroid of about 50 m or more in diameter is hazardous to life on Earth. In 2006, there were about 340,000 known asteroids and comets and about 700 known NEOs with diameters greater than 1 km; current estimates now list 1,100 NEOs with diameters greater than 1 km and approximately 100,000 NEOs with diameters

greater than 140 m. The current list of PHOs contains roughly 800 objects (NASA Report to Congress, 2007).

Applying a sustained force over a long time is considered a more controllable way to change the orbits of small NEOs (tens of meters in diameter to ~100 meters in diameter) and larger NEOs en route to keyholes than detonating high-energy weaponry at the target (National Research Council, 2010), if sufficient time is given. However, it also requires mastering yet-to-be-developed space technologies on unprecedented scales (Ahrens, 1992). Among the concepts being advanced are gravity tugs using massive spacecraft and irradiation of the asteroid surface to produce jets of materials. The former requires launching a spacecraft with a mass in excess of tens of tons and flying it on a precise course to the target for nearly a decade. Irradiation works by focusing lasers or solar beams on the object's surface to sublime surface minerals, thereby creating outgoing jets capable of imparting a propulsive momentum to the asteroid. Such concepts are attractive in principle, but run into significant obstacles that raise doubts about their implementation: (1) solar collectors with diameters on the order of hundreds of meters must be flown in precise formation with a rotating NEO, and (2) the sublimated material ejected is likely to contaminate the optics of the system over time. Other recent studies (Olds, 2007) describe fleets of landers equipped with mass drivers capable of drilling and ejecting materials from an asteroid to generate the needed propulsive force.

5. FEASIBILITY: ENERGY REQUIREMENTS FOR ICE UTILIZATION

This study focuses on assessing the feasibility of using sublimation of frozen volatiles or the volatilization of mineral oxides to generate gases to produce mechanical work at various planetary bodies.

5.1 Sublimation of Ice in the Solar System

The wide range of locations where water (H₂O) and CO₂ ice has been discovered throughout the Solar System focuses our attention on these materials (Table 1). The phase diagrams presented in Figures 1 and 2 display the conditions of both water and CO₂ on various planetary and other solid bodies.

Table 1. Molecules detected as ices on outer solar system planets and satellites*

| Planet | Satellite | Ices (molecules) detected |
|---------------|------------------|---|
| Jupiter | Io | SO ₂ , SO ₃ , H ₂ S (?), H ₂ O (?) |
| | Europa | H ₂ O, SO ₂ , H ₂ O ₂ , CO ₂ |
| | Ganymede | H ₂ O, O ₂ , O ₃ , CO ₂ , SO ₂ |
| | Callisto | H ₂ O, CO ₂ , SO ₂ |
| Saturn | Titan | H ₂ O, CO ₂ |
| | Mimas | H ₂ O (?) |
| | Enceladus | H ₂ O |
| | Tethys | H ₂ O |
| | Dione | H ₂ O, O ₃ |
| | Rhea | H ₂ O, O ₃ |

| Planet | Satellite | Ices (molecules) detected |
|---------|-----------|---|
| | Hyperion | H ₂ O |
| | Iapetus | H ₂ O, H ₂ S (?) |
| | Phoebe | H ₂ O |
| | [Rings] | H ₂ O |
| Uranus | Miranda | H ₂ O |
| | Ariel | H ₂ O |
| | Umbriel | H ₂ O |
| | Titania | H ₂ O |
| | Oberon | H ₂ O |
| Neptune | Triton | N ₂ , CH ₄ , CO, CO ₂ , H ₂ O |
| Pluto | (itself) | N ₂ , CH ₄ , CO, H ₂ O |
| | Charon | H ₂ O, NH ₃ |

*From Cruishank et al., 1998.

Favorable conditions for sublimation are found in vacuum or rarefied atmospheres on satellite moons, comets, and asteroids (such as Ceres) where water ice is present. By contrast, the dense atmosphere of Titan rules out sublimation of water ice. On Mars, a permanent polar cap of water ice is an attractive resource, but sublimation may require more complex engineering as the conditions hover around the triple point. These initial considerations must be examined further in future work through experimental testing of CO₂/H₂O ice mixtures that are contaminated with embedded regolith dust grains.

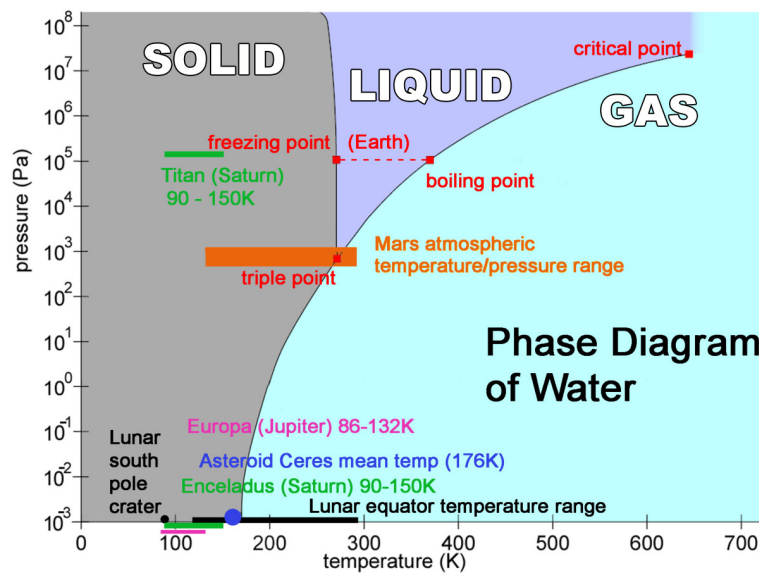


Figure 1. Phase diagram of water with conditions existing in the Solar System

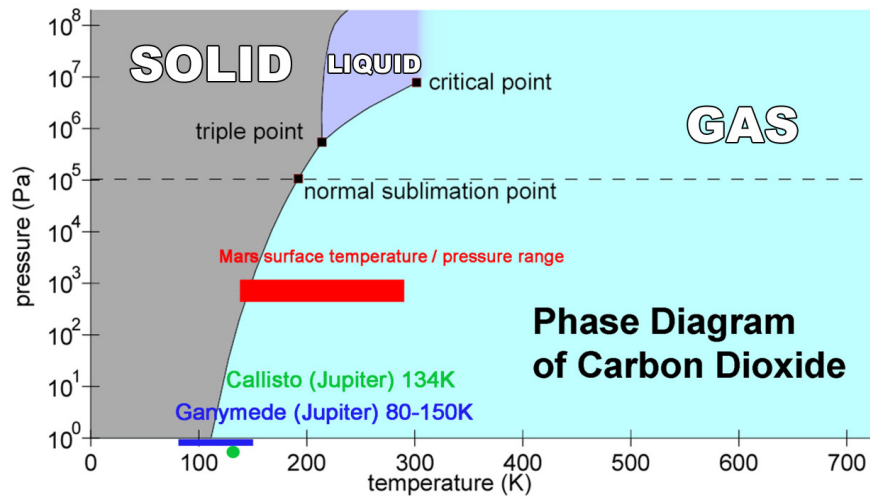


Figure 2. Phase diagram of CO₂ with conditions existing in the Solar System

The thermodynamic states of these compounds in their environment establish the minimum energy requirements for any phase change, either through sublimation or liquefaction. The enthalpy of sublimation of water in a lunar environment taken as example (173 K or $-100\text{ }^{\circ}\text{C}$, 7.5×10^{-9} torr) is on the order of 2.82 MJ/kg, equivalent to 783 Wh/kg (see Figure 3). When mixed with 6 vol.% of lunar regolith (sample composition from Apollo 15), the enthalpy value is calculated to be 3.12 MJ/kg (867 Wh/kg) when the heat capacity (C_p) of both pure ice and regolith are weighted by volume (see Figure 4).

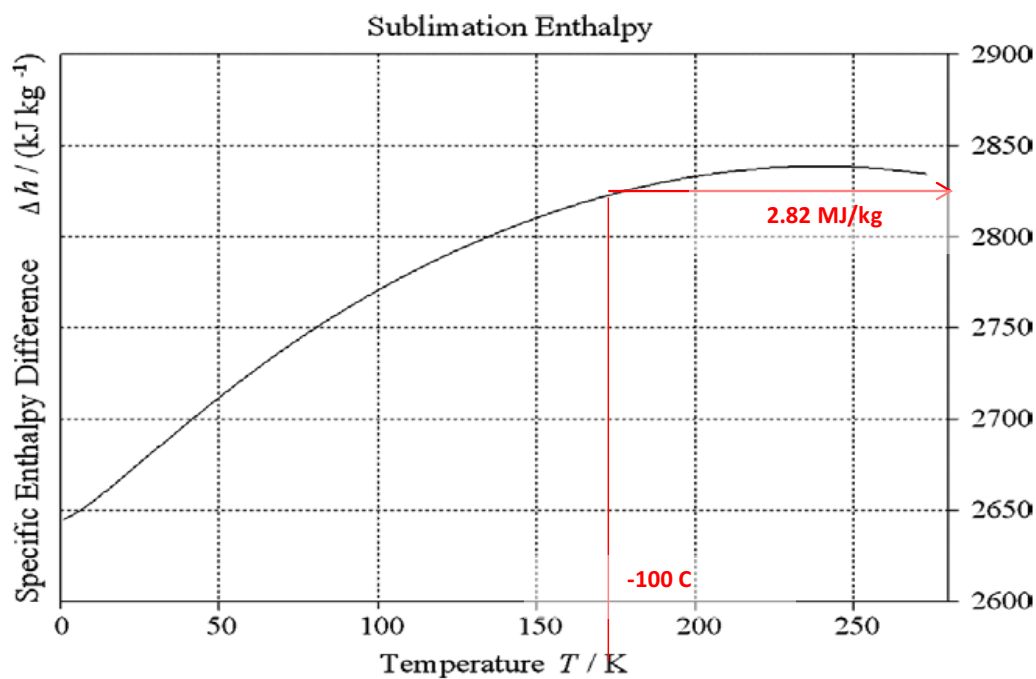
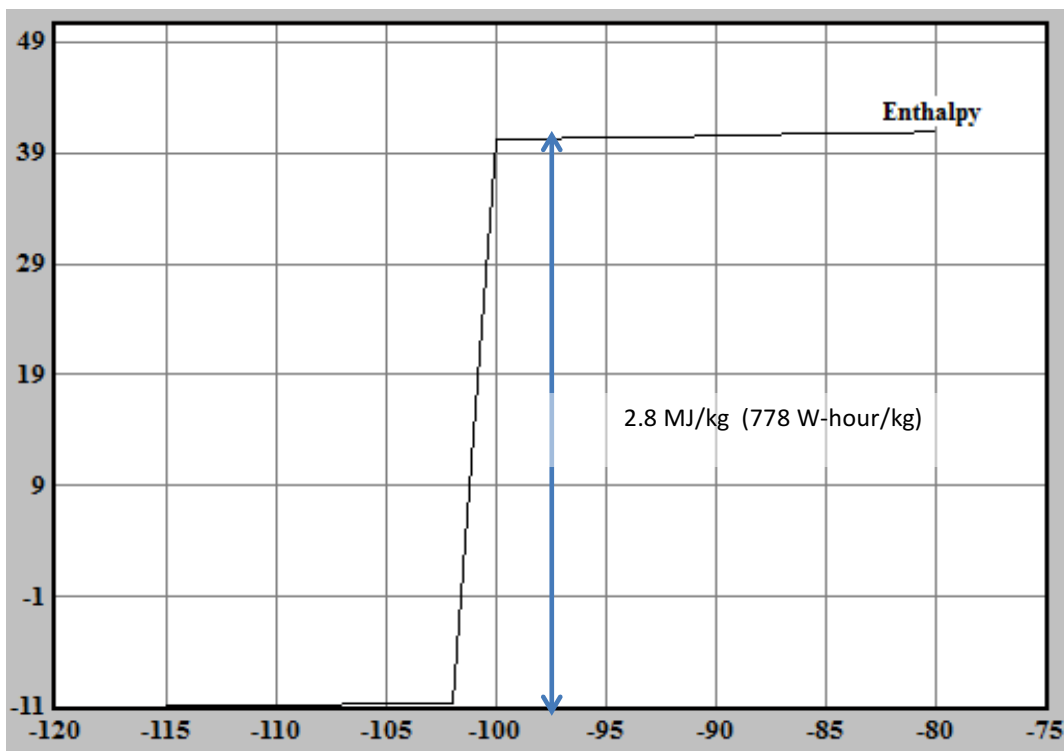


Figure 3. Enthalpy of sublimation of H₂O at 7.5 × 10⁻⁹ torr: (a) Calculated using HSC Chemistry and (b) reported from Feistel et al., 2007

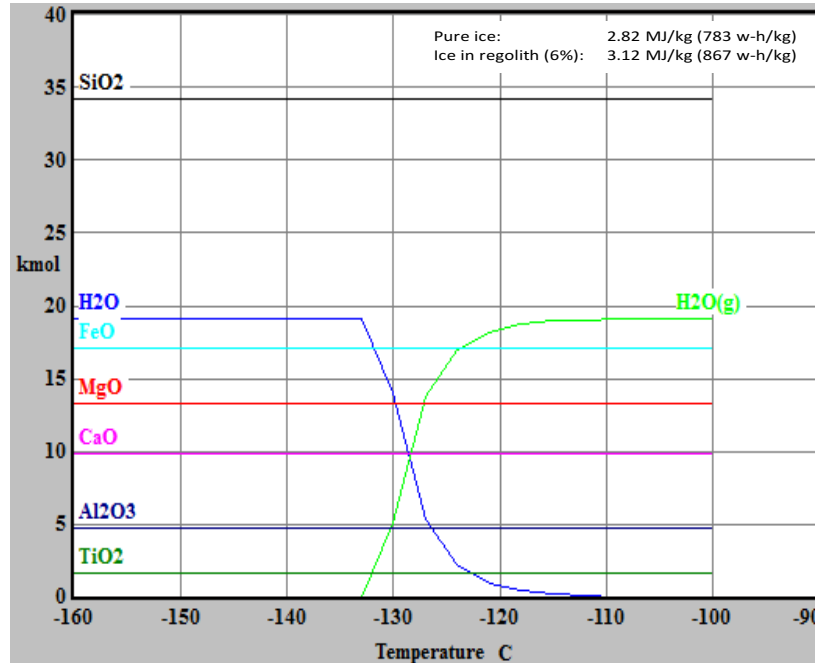


Figure 4. Enthalpy of sublimation of water ice mixed with regolith

Values are calculated in HSC Chemistry using a mixture of pure ice and 6 vol. % of granular material with composition of an Apollo 15 sample.

Sublimation conditions and rates for water at very low temperatures and pressures have been investigated in greater detail in the past decade to understand the evidence of lunar ice provided by lunar orbiters (Andreas, 2007). We used this data to build a useful phase diagram for the propulsion model described later. In Appendix A, we have identified in a graphical manner the thermodynamic regions of existence of water ice on planetary surfaces of interest. The lunar poles and shadowed craters under temperatures from 40 K to ~125 K provide a thermally stable environment for water ice to accumulate and similar conditions exist on comets. On Mars, water finds stable regions but often teeters around its triple point, where it may oscillate between solid, liquid, and gas (A.3). Water ice finds very auspicious conditions on Europa to blanket the surface of this fascinating world; under a tenuous oxygen atmosphere (10 torr), the moon of Jupiter has built a massive crust of water ice several kilometers thick that may hide a vast water ocean. Farther, near Saturn, Titan offers excellent conditions for ice stability, but this time under an atmosphere of nitrogen 1.5 times denser than ours. On Titan, water ice would melt as it does on Earth when heated on the surface.

The Martian environment is dominated by the ~95% CO₂ atmosphere and its changing surface temperatures. The phase diagram of pure CO₂ indicates that a relatively small amount of heat should suffice to sublimate this ice. Under similar conditions, the enthalpy of sublimation of CO₂ is on the order of 0.44 MJ/kg, equivalent to 121.4 Wh/kg. Experimental data under these conditions confirm that radiative transfer between the warmer Martian atmosphere and the surface ice is enough to sublimate the latter (Blackburn, 2008). Future experiments on ice mixtures with CO₂, H₂O, and regolith should be done to observe how such mixtures behave differently than pure substances. Appendix B displays the regions of existence of CO₂ on selected planetary surfaces across the Solar System. While several authors have published data on the phase diagram at low temperatures and pressures, it does not extend low enough in pressure to cover the conditions on the Moon; we performed an extrapolation by curve fitting the existing data to establish values in that area and use them in the models (B.1). Carbon dioxide ice is stable in shadowed areas of the Moon and in comets but its volatility enhances sublimation in both locations. This compound is found in comet tails as these objects approach the Sun. Under different conditions, Europa and Titan both support the existence of CO₂ ice although no data has been reported of its presence on Titan.

The worlds of the outer planetary systems are bathed in such cold temperatures (near 50 K or -223 °C) that methane (CH₄) and nitrogen (N₂) ices dominate on the surface of Pluto (Cruishank, 2013) along with carbon monoxide and coexist with water (H₂O) ice on several moons of Uranus such as Ariel, Oberon, Titania, and Umbriel. Water and ammonia (NH₃) ices have been detected on Pluto's moon, Charon (Cruishank 2013). Methane also is a major part of the environment of Titan, the largest satellite of Saturn; hundreds of lakes of methane have been counted in observations made by the Cassini probe and methane rains seem to occur in polar regions in a dense lower troposphere of ~95% N₂ and ~3% CH₄. We employed the same approach to extrapolate existing data for the phase diagram of CH₄ into regions of extreme low pressures and temperatures at various planetary surfaces in Appendix C. The results reveal that CH₄ is not likely to be present as ice anywhere on the Moon since the solid-gas equilibrium line tracks below the lowest temperature of 40 K (-233 °C) reported on the Moon (C.1.) A similar situation applies to cometary or asteroid surfaces where methane is not expected for the same reason (C.4.) In environments where the atmospheric pressure reaches a few torrs in value, CH₄ ice forms and such is the case on Mars and Europa (C.3, C.5 respectively.) Uniquely, CH₄ is found as a liquid on Titan's surface (C.6) where it participates in a methane cycle similar to our own water cycle. is also a minor component (~1.4%) in the lower atmosphere and a major component of the surface materials of Titan, which was visited by the Huygens probe (Niemann, 2005.) Energetically, The CH₄ enthalpy of vaporization at 100 K is 0.53 MJ/kg or 147.2 Wh/kg (Frank, 1937) and the enthalpy of sublimation at 67-88 K is 0.6 MJ/kg or 166.7 Wh/kg (Stull, 1947.) The enthalpies do not change along a given phase-change line. From the sole perspective of energy expense, resources such as ices of CO₂ and CH₄ are much preferable over H₂O ice and could be preferred if the resources are co-located and similarly accessible. Accessibility is the key factor here since many planetary surfaces harboring CO₂ and CH₄ ice also are also covered in H₂O ice. While CO₂ is soluble as a gas in water, it is only liquid at pressures above 5.1 atm which are not found near the surface of any rocky planet, moon or asteroid in the Solar System. This suggests that CO₂-H₂O ice may be co-mixed during their

formation at very low temperatures and CH₄ also finds its way in the water crystal lattice in the form of clathrates. When these icy compounds are found as mixtures, the minimum energy that must be expended to sublimate them would be that of H₂O.

5.2 Volatilization of Mineral Oxides

While ice and other volatile compounds are found on and below the surface of many objects of our Solar System, many interplanetary surface missions will encounter dry rock and regolith bodies. A majority of objects in the inner part of the asteroid belt appear to be devoid of ice, while those in the outer orbits may be icy (Levison, 2009.) Several moons of Uranus and Neptune also appear to be dry. On the surface of such bodies, gas production is possible by either evaporating the oxides of the rocks after heating the minerals above their melting points or by separating the oxygen from the bound elements that compose the oxides. Vacuum pyrolysis of mineral oxides, such as silicates, melts the oxides and separates the oxygen from the metal elements via direct heating of the mixture under vacuum which is the most prevalent condition of the targeted destinations. The melt components evaporate or ablate according to their enthalpy of vaporization. The gas thus produced contains monoatomic and diatomic species that undergo some recombination and condensation quickly after release. Figure 5 displays an example of the evolution profile over temperature of the major molecular and atomic components found in regolith of composition similar to those found on the lunar surface. The calculations are made for an ambient pressure of 10⁻⁷ torr and show that molecular dissociation and vaporization occurs over a wide range of melt temperatures. Major components of the regolith like silica (SiO₂) and ferric oxide (FeO) dissociate into gaseous compounds around 1,200 to 1,400 °C followed by alumina (Al₂O₃) near 1,600 °C. Theoretical treatment of the dynamics of a Knudsen layer formed within a few mean free paths of the liquid-gas interface revealed that mass flow rates of monoatomic gas receiving high density energy inputs achieve sonic or supersonic conditions under hard vacuum (Knight, 1979.) Although such model was built for monoatomic surfaces interacting with laser radiation, the physical phenomenon of rapid evaporation is intriguing when applied to the surface of a rock in the vacuum of space. Under laser radiation, molten material brought to temperatures nearing 1,400 °C and very high vacuum, the kinetic energy gained by the volatilized species may produce a significant thrust if the molecules are directed in their escape of the surface. This concept of laser ablation for PHOs deflection was first advanced by Melosh et al. (Melosh, 1994.) The cumulative energy levels required for various targets have led several authors to propose and evaluate missions performed by single spacecraft stationed near the target while irradiating it with megawatt-class (one to 50 MW) lasers powered by nuclear reactor with mixed conclusions (Phipps, 1997; Park and Mazanek, 2005.) More extensive studies have recently been conducted that propose concepts of multi-spacecraft carrying kilowatt-class lasers working in swarms to deflect an asteroid using this principle (Vasile, 2010.) Experimental validation of such concept undertaken by researchers of the University of Strathclyde (Gibbins, 2012) provided ejecta mass flow rates of the order of 2x10⁻⁷ kg/s at velocities ~ 1,130 m/s using a 62W laser on the mineral olivine. The corresponding thrust values calculated by the authors predict that a fleet of ten spacecraft working in concert to focus their combined 22 kW laser beams on the same spot on a 250 m diameter

asteroid for nine years would deflect the target by 10,000 km off its path and avert potential impact with Earth. The authors also describe an alternative mission concept where the swarming spacecraft concentrate the beams of 1 kW solar-pumped lasers additively while flying in formation with the asteroid. Direct measurements of flow rates with other materials and textures and the effects of laser defocusing by the ejected material are main issues to understand in future experimental work that surely will refine the deflection models. However, execution of this concept is very challenging at best; the volatilization of oxygen alone (40-50% by weight of several known regolith) under these conditions requires a large energy expenditure with values on the order of 12 MJ/kg (i.e., 4.7 kWh/kg) leading to cumulative energy values on the order of 10^4 GJ required to move targets with diameters ranging from hundred meters to one km as found by Park and Mazanek. Although the deteriorating effects of the contamination of the optics (laser and solar collectors) on resulting thrust are acceptable, these mission scenarios require continuous focusing of powerful pulsed lasers on target for months at a time. The referenced studies have not yet included the spin and nutation characteristics of the asteroid that directly impact the feasibility of such operations. Large numbers of asteroids spin with periods ranging from less than one hour to several hours.

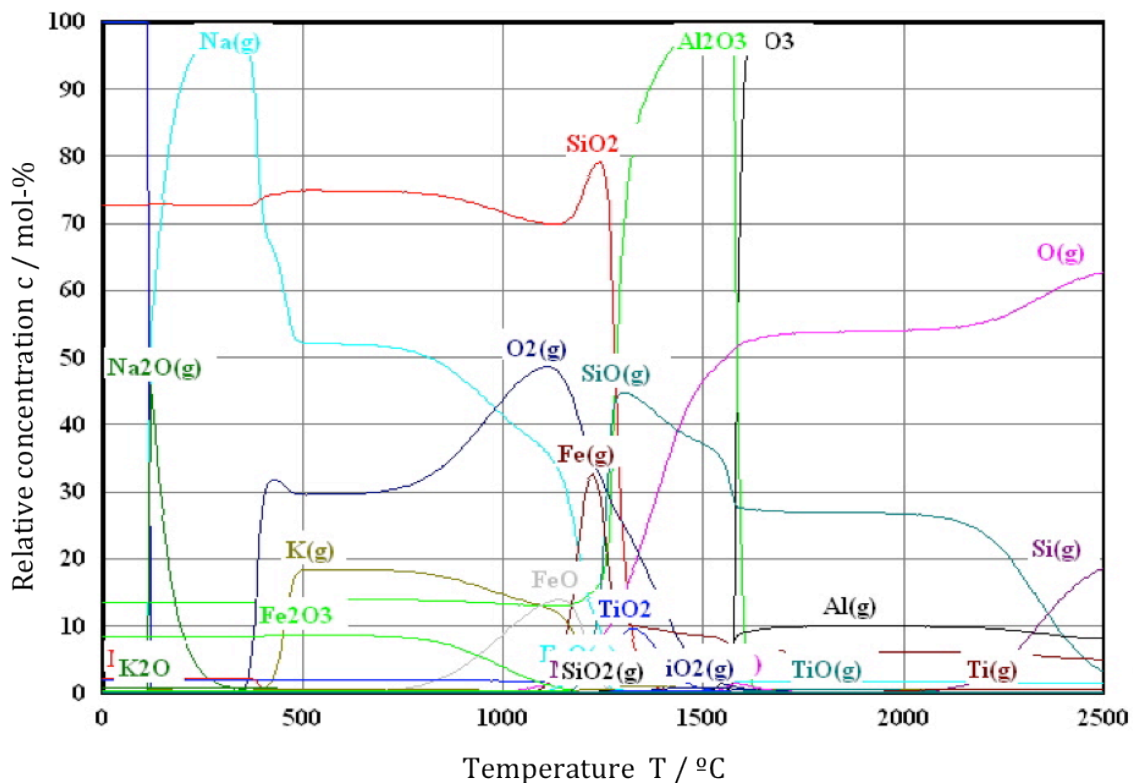


Figure 5. Evolution of gaseous specie from a pool of molten regolith under vacuum conditions (10^{-7} torr)

Calculations performed with HSC Chemistry.

5.3 Excavation and Collection of Ice Resources

The use of volatile solids for power applications begins with their excavation, usually in the form of icy regolith that contains an amount of regolith by percentage of mass that varies from 0% (pure solid volatile) to 100% (pure mineral). The icy regolith may consist of ice-encapsulated regolith particles in which the individual icy regolith particles are either not bound to one another or loosely bound together, or as a solid volume of ice and regolith. It is also possible for a solid rock to be permeated with a volatile substance in the form of a gas, liquid, or solid depending on the temperature and atmospheric pressure of the local environment.

Rock strength depends on temperature as well as pressure. The higher the temperature, the more plastic the rock is. By contrast, the lower the temperature, the greater the strength of the rock, especially when the rock contains significant amounts of water. The freezing effect of water within the pores of a rock increases the rock strength until a difference in the thermal coefficient of expansion causes a differential strain between the rock and water ice that leads to a weakening of the rock. It is observed that the gradual increase in strength as the temperature of the rock decreases reaches an upper limit around $-120\text{ }^{\circ}\text{C}$. By comparison, the average surface temperature of an asteroid may be $-70\text{ }^{\circ}\text{C}$, while the temperature on a comet may vary from $-113\text{ }^{\circ}\text{C}$ in the shadow of the sun to $-44\text{ }^{\circ}\text{C}$ near the sun. Temperature is about $-230\text{ }^{\circ}\text{C}$ within a permanently shadowed lunar crater at the Moon's south pole. On Mars, surface temperatures can decrease to $-140\text{ }^{\circ}\text{C}$ to $-150\text{ }^{\circ}\text{C}$ at the poles (Mars Facts, 2012).

Thermal spalling (Figure 6) causes solid rock to fracture into smaller fragments that can be more easily excavated. This approach uses solar energy to heat a rock to a temperature between $400\text{ }^{\circ}\text{C}$ and $600\text{ }^{\circ}\text{C}$ that results in thermal stresses created by a mismatch in the thermal expansion of the mineral components and grains within the rock structure (Zacny, 2009). Thermal melting occurs in the higher temperature range between $1,100\text{ }^{\circ}\text{C}$ and $2,200\text{ }^{\circ}\text{C}$, which results in the direct vaporization of the minerals in the heated regolith and rock, including any volatiles that may be present.

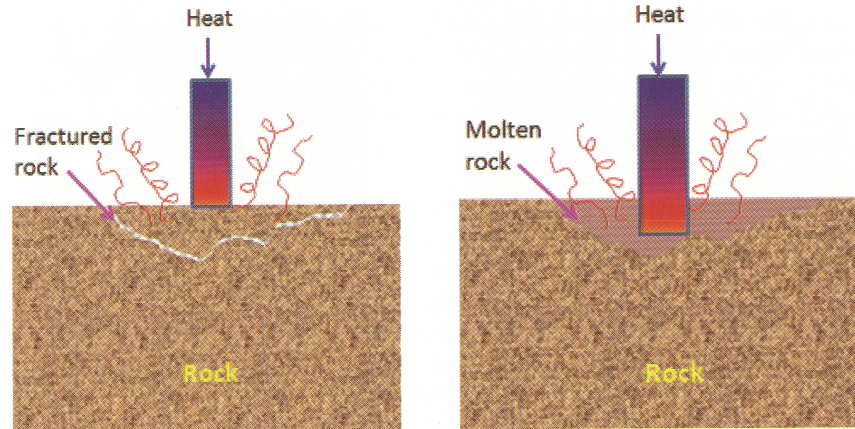


Figure 6. Thermal spalling (left) involves thermally fracturing a rock formation. Thermal settling (right) involves the melting and evaporation of a rock formation.

From Zacny, 2009, in “Mars: prospective energy and material resources”, Badescu, V. Ed., Chapter 15.

Assuming that the volatile solids are to be found in the form of icy regolith, the possible methods of accessing the volatiles contained in loose regolith may involve scooping, drilling, pneumatic excavation, or the direct extraction of volatiles by injecting heat into the icy regolith and then capturing the volatile by some means, such as refreezing the volatile on a cold surface. Rice and co-workers proposed three systems to accomplish the extraction of water ice and hydrogen in lunar regolith out of permanently shadowed craters in a NIAC study (Rice, 2000); (1) Direct heat input into ice-rich regolith by a microwave generator with above-surface freezing and transport of re-frozen ice by a H₂O fuel cell-powered rover, (2), in-crater mining and processing of ice in a furnace followed by steam transport in heated pipes, and (3) surface mining by drag-bucket lines of the crater regolith for processing in solar furnace. The authors did not identify a preferred method but indicated that the selection would critically depend on nature and concentrations of the deposits and their scale including their distance to sunlit areas for power availability. Both photovoltaics and RTGs were considered as power sources.

Scoops offer a simple yet robust method of acquiring small to large amounts of loose regolith. They also provide a means of geotechnical testing of soil by measuring the bearing strength of the top soil and determining excavation forces. The problem with scoops is that they are hindered by the presence of highly compacted soil, rocks, and hard icy regolith. Some of these problems can be alleviated by adding a percussive force to the scooping action.

Drills are able to penetrate rocks and ice, but have difficulty with accumulating large amounts of regolith. When a drill is used in a remote location under extreme environmental conditions, it is necessary to remove the cuttings from the hole that is being drilled. An auger is usually used to remove cuttings, although sublimated gas resulting from frictional heating may also be used. Difficulties involved with using drills include the so-called “drill walking” when rocks are encountered, and an undesirable

amount of heating that can melt volatile solids and cause them to refreeze on the drill bit. Percussive drilling is increasingly being used for planetary missions because of the significant increases in drilling rate.

Whether scoops or drills are used to collect icy regolith, methods of handling the presence of rocks in the regolith must be considered since highly efficient regolith excavation results in less time spent operating in an extreme planetary environment. Autonomous robotic excavation operations are clearly required because of the long communication time delays that would be encountered by teleoperated robotic excavators.

It is also possible to combine a drill with a scoop to take advantage of the benefits that each method provides. The Phoenix Mars Lander mission included an Icy Soil Acquisition Device (ISAD) that combined a scoop with a drill-like device called a RASP that was able to penetrate the hard frozen soil near the lander using 30 W of power. The scoop could exert 1170 N of digging force and collect up to 310 cm³ of regolith (Zacny, 2009.)

Percussive scooping or shoveling has demonstrated a reduction of the digging force required by a factor of 15–25 over nonpercussive scooping. Terrestrial earth-moving equipment relies on shear force to excavate soil, but in a reduced gravity environment where lightweight digging equipment must be used, percussive scoops offer the advantage of less reliance on the weight of the equipment to provide the reaction force needed to scoop regolith (Zacny, 2009.)

Pneumatic excavation (see Figure 7) is a recent development that is made feasible by the volatilization of residual propellant that may remain onboard a planetary lander vehicle after landing.

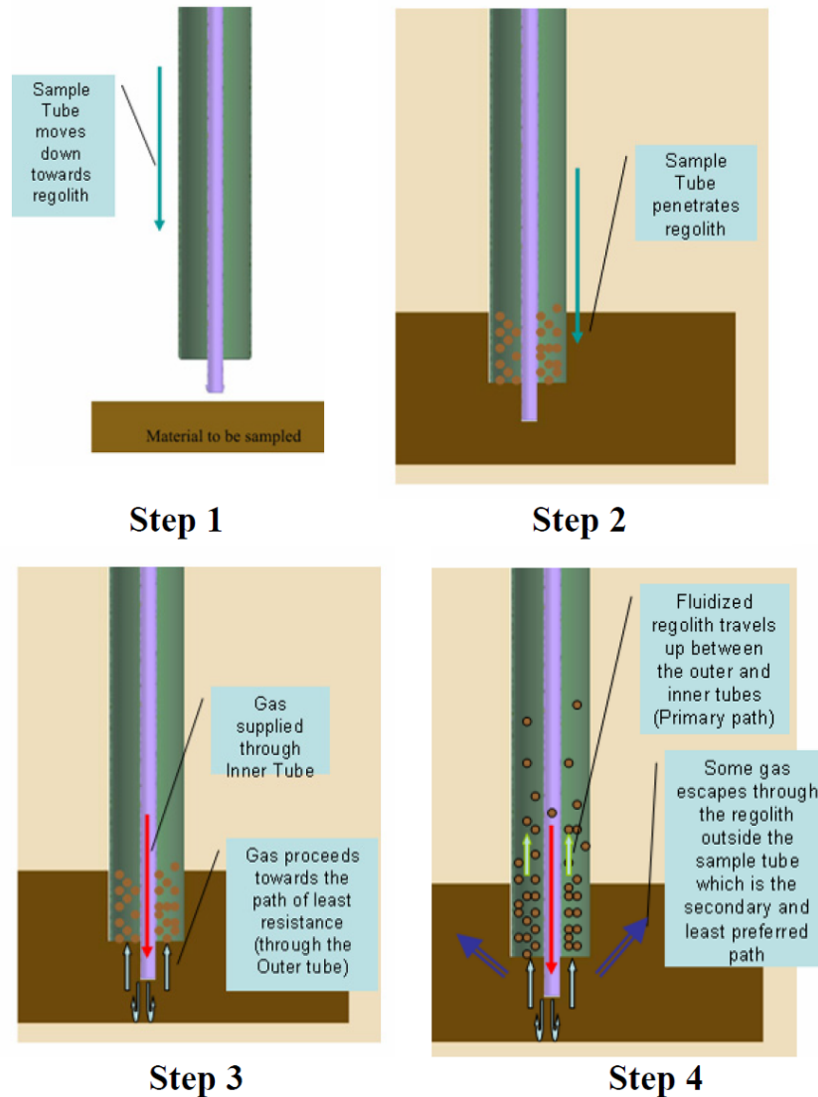


Figure 7. Operational steps in the plunge method for pneumatically excavating and lifting regolith

From Bar-Cohen & Zacny, 2009, "Drilling in Extreme Environments," Chapter 6.

The excavation method uses two coaxial tubes to inject compressed gas down the center tube that is embedded into surface regolith. This results in the lifting of regolith, which then flows upward along the outer annular tube and is collected in a storage container. Tests have been conducted under low pressure conditions (chamber at 1 torr) using 1 gram of gas (air at 1 atm) to lift 3,000 grams of lunar regolith simulant JSC-1A (Zacny, 2009.)

Sublimated volatiles may also be used to excavate regolith. The Martian environment is unique because its atmospheric pressure ranges from 0.1 kPa to 1.5 kPa, which bounds the triple point of water at 0.63 kPa and 0 °C. If the pressure is slightly below the triple point of water, then a temperature increase above 0 °C will result in sublimation. Laboratory drilling experiments conducted under simulated Martian atmospheric conditions (Zacny, 2004) demonstrated the effect that water ice sublimation can have upon drilled chips from a rock sample. The frictional heat that developed during the drilling operation was enough to heat up the drill bit and rock so that it caused water ice within the rock to sublimate. The volumetric expansion of water ice into water vapor was about 100,000 times, and resulted in the drilled chips being blown out of the borehole.

This sublimation effect could also be used to directly extract water from icy regolith (Mungas, 2006). In regions on Mars where the atmospheric pressure exceeds the triple point of water, an optically transparent enclosure placed on the surface can trap heat from incident solar radiation, thus warming up the icy regolith as shown in Figure 8. When the water ice sublimates, trusses inside the enclosure act as cold fingers that allow the water vapor to condense. Each truss connects to a water collector where the water can be pumped into a storage container.

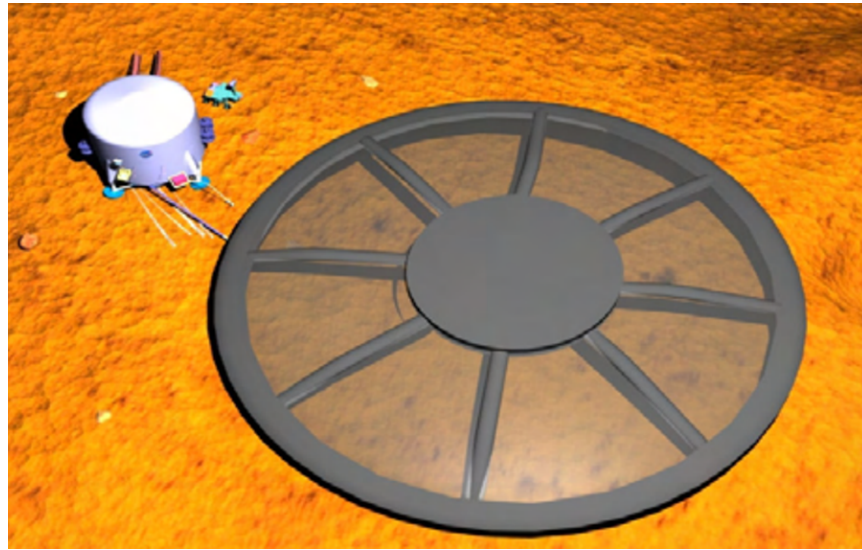


Figure 8. Notional deployable cover for enhancing surface optical properties as well as providing a collection volume for collecting cold steam. (Mungas, 2006)

6. FEASIBILITY: POWER OUTPUTS FROM SUBLIMATED ICE GASES

6.1 Propulsion

Cold gas propulsion is one of the three most common propulsion systems, the others being monopropellant and bipropellant propulsion. While all have been demonstrated in spaceflight, cold gas propulsion offers particular advantages when low total impulse values are needed and system mass must be kept low. In fact, it has been shown to be the most efficient option below 200 s of impulse value (Figure 9).

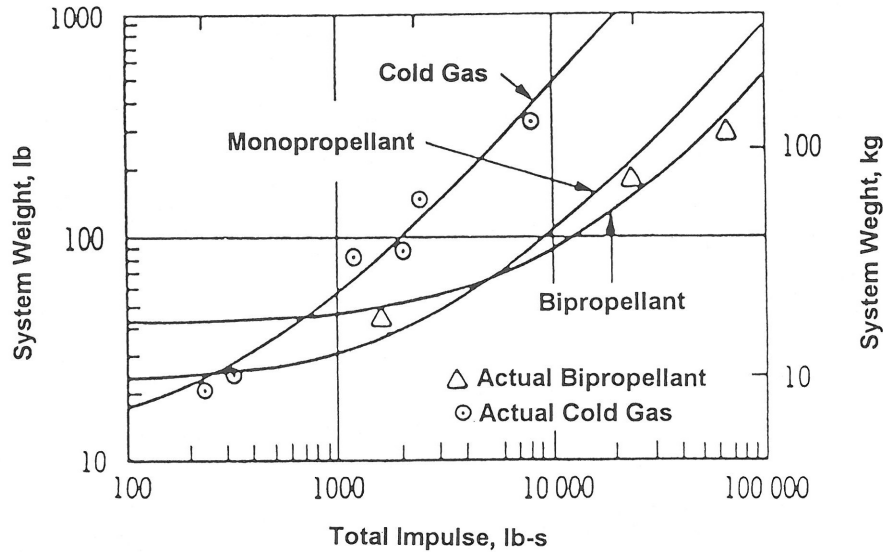


Figure 9. Comparison of common propulsion systems based on actual system mass and total impulse generated (Brown, 1996)

For a given total impulse, the more efficient system has the least mass.

Vernier thrusters have been one of the main applications of cold gas propulsion; one of the latest examples is the SPHERES spacecraft using CO_2 aboard the International Space Station (ISS) (Mohan, 2009.) Cold gas systems offer great simplicity because they typically require only propellant tanks, filling and relief valves, plumbing (feed lines, filters, and sometimes line heaters), a pressure regulator (except in a blowdown system), and thrusters (including control valves and nozzles).

6.1.1 Thrust Model

Modeling achievable thrust using the various gases produced *in situ* was done using a model created in COMSOL Multiphysics. Since the objective is to examine the feasibility of using specific gas resources in their planetary environment, the model was kept simple to allow direct comparisons of the cases. As shown in Figure 10, the 3D spatial domain created for this study consists of a cylindrical tank, a throat, and a nozzle allowing the gas to expand into a volume at set ambient conditions.

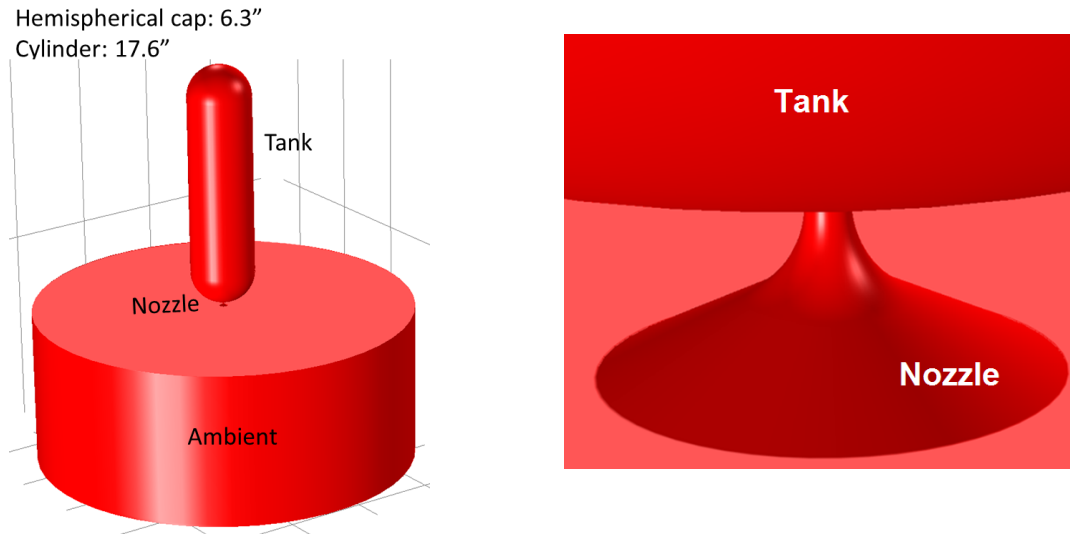


Figure 10. 3D spatial domain used in the thruster model to compute thrust performance of carbon dioxide, methane, and water steam

This simplified transient model is based on the analysis of the conditions at three distant points along the thruster gas flow. The first point is located at the gas stagnation section of the tank farthest away from the nozzle, the second point is located at the pressure regulator that controls the nozzle inlet pressure (and as a consequence, the thrust yielded by the nozzle), and the third point is located at the exit edge of the nozzle. Figure 11 illustrates the 2D domain (Figure 11a) and location of the three flow points (Figure 11b). At point #1, the gas velocity is assumed to be zero all the time (gas stagnation) and P_0 and T_0 are the transient pressure and temperature at that point. At point #2 (the pressure regulator), the pressure remains constant with time while velocity (V_1) and temperature (T_1) are the transient variables. At point #3 (the nozzle's exit plane), the pressure is set to equal the ambient pressure (case of optimum expansion) and the gas velocity (V_2) and temperature (T_2) are the transient variables.

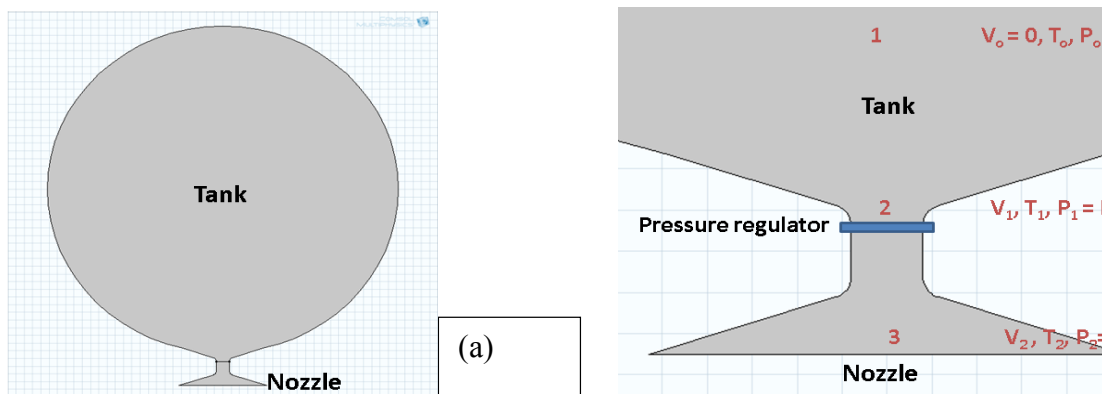


Figure 11. 2D domain (a) and gas flow location points (b) used in the simplified transient thrust model

The gas behavior is nonideal at high pressures, and this occurs in this system for a short interval after the start of the expansion until the tank pressure is low enough to resume treatment as an ideal gas. The real gas behavior is modeled through the use of the Redlich-Kwong equation of state and numerical solutions for the variables are computed at intervals during that phase. We built lookup tables showing the compressibility factors of several gases at the operating conditions selected in the study to yield high thrust. At 3,000 psia and higher, the compressibility factor of the gases we are using have values between 1.4 and 1.6, meaning that the deviation in gas density (in the first instants of the expansion) with respect to ideal gas is substantial. The fundamental relations that link these three points and allow us to determine their flow conditions (velocity, pressure, and temperature) in transient mode are described below.

Energy equation:

$$\frac{v^2}{2} + h = \text{constant} \quad (1)$$

where v is the velocity of the gas, and h the enthalpy of the gas.

Entropy (thermodynamic second law):

$$Tds = dh - \frac{dp}{\rho} \quad (2)$$

where T is the temperature, s the entropy, p the pressure, and ρ the density of the gas.

Mass balance ($v \neq 0$):

$$v\rho A = \text{constant} \quad (3)$$

where A is the cross-section area of the tube section through which gas is flowing.

Ideal gas equation:

$$\rho = \frac{P}{RT} \quad (4)$$

where R is the ideal gas constant.

Assuming a reversible/isentropic gas expansion and ideal gas behavior allows us to express Equation 2 in terms of temperature and pressure by substituting $ds = 0$ (isentropic) and $dh = C_p dT$ (ideal gas). Equation 3 now can be replaced by equation 3'.

$$C_p dT = \frac{dp}{\rho} \quad (3')$$

Where C_p is the heat capacity at constant pressure.

We still need the relation that yields the transient change of mass at the tank as the equations listed above (1 through 4) are state-state flow conditions. This equation is derived from the transient energy balance at the tank as expressed in equation 5.

$$\frac{dm}{dt} = v_2 \rho_2 A_2 \quad (5)$$

where m is the mass of the gas in the tank; t is time; v_2 gas velocity at the nozzle; ρ_2 is the gas density at the nozzle; and A_2 is the nozzle cross-sectional area perpendicular to the gas flow.

m can be expressed in terms of pressure and temperature using the ideal gas equation and used in equation 5 to yield:

$$\frac{M_w V}{R} \left(\frac{1}{T} \frac{dP}{dt} + P \frac{d\frac{1}{T}}{dt} \right) = v_2 \rho_2 A_2 \quad (5')$$

where M_w is the molecular weight of the gas; and V is the volume of the tank.

The set of equations 1 through 5 is solved numerically to determine the transient values of pressure, temperature, and velocity at the 3 points and be able to determine thrust with time. The thrust can be calculated as:

$$F = \frac{dm}{dt} v_2 + (P_2 - P_a) A_2 = (\rho_2 A_2) v_2^2 + (P_2 - P_a) A_2 = A_2 [\rho_2 v_2^2 + (P_2 - P_a)] \quad (6)$$

where P_a is the ambient pressure in which the gas expands at the nozzle exit plane.

We used the thermodynamic parameters from phase diagrams shown in the appendices and other published data to investigate the conditions of gases such as water vapor, CO₂, and CH₄ necessary to yield thrust while avoiding condensation or freezing inside the thrusters. Examples of these results are discussed further in Section 7.1.

6.2 Pneumatics

Actuation of machinery is the second use of the potential energy stored in the evolved gases from sublimation of ice. The magnitude of force needed from the actuator dictates the required gas pressure to be achieved in the cylinder. The ambient conditions in which the work is performed may constrain the mechanism by limiting the range of expansion of the gas to avoid liquefaction or freezing of the gas.

The gas produced by sublimation is stored at pressure in a source tank. It is introduced into the piston chamber through a valve and expands to produce work. Once expanded, the gas can be collected into a second tank maintained at low ambient pressure set by the

surrounding environment. That filling process can be performed several times by keeping the tank cold to keep the pressure low. The tank temperature can be maintained by directly exposing it to the surrounding environment, which could freeze the gas once again. The second tank is then used as a source tank for the pneumatic system.

Experimental work has demonstrated that air, CO₂, or other gases such as N₂, can be effectively used to excavate and transfer large masses of regolith while recycling these gases.

6.2.1 Pneumatic Transport of Solids Using Martian CO₂

A two-phase (solid-gas) flow model was built via a Computational Fluid Dynamics (CFD) approach to forecast process requirements to pneumatically transport granulated material using Martian CO₂ as the gas carrier. The interconnected units considered in this pneumatic process include a hopper, an eductor, a riser, a cyclone, pressure regulators, and pipe line segments to connect these units as illustrated in Figure 12.

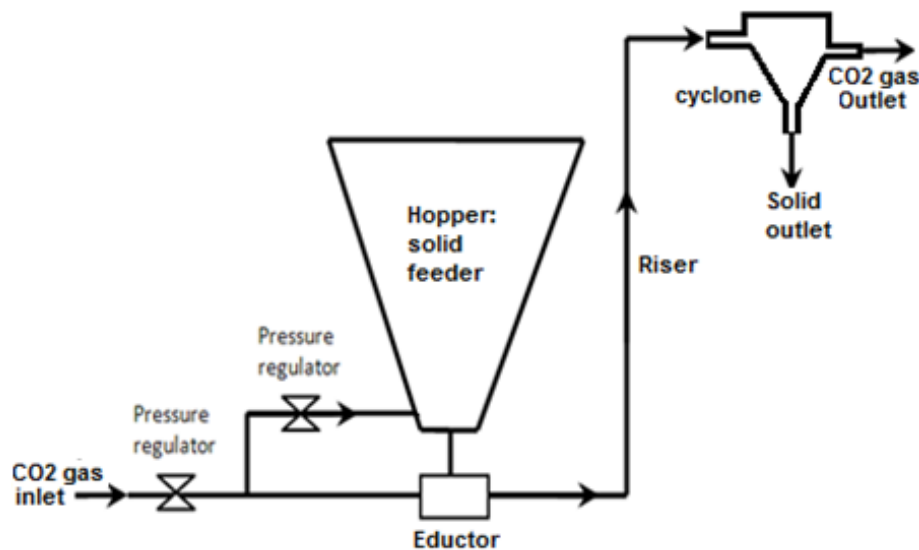


Figure 12. Assembly and connectivity of the operational units used to pneumatically transport Martian material using CO₂ gas

CO₂ gas is injected into the eductor, which is also connected to the hopper. The hopper is used as a feeder of the granulated material, creating a differential pressure that thrusts the granulated material at the hopper toward the CO₂ gas that is flowing through the eductor to mix it and pneumatically transport the granulated material along the pipe and elevate it through the riser. The key unit in the process is the eductor because it is where the material flow rate is originated by setting the gas pressure at the eductor inlet and the pressure inside the hopper. The model was validated using air as a gas carrier and used the results to forecast the performance of pneumatic transportation of Martian granulated material via CO₂ gas instead of air. An experimental setting was assembled using a commercially available eductor that is vertically connected to a hopper unit filled with

regolith Simulant JSC-1A. A single inlet gas flow rate was set and the respective particle flow rate was measured during the entire hopper evacuation.

6.2.2 Solid-Gas Flow Model: Fundamentals

Several different modeling approaches for solid-gas flow modeling have been developed, ranging from discrete, particle-based methods to macroscopic, semiempirical, two-phase descriptions. Particle-based methods are suitable when there are a limited number of solid particles. When there are many particles, it is better to use a macroscopic, or averaged, model that tracks the volume fractions of the phases.

The numerical simulation of fully developed gas-solid flow at the eductor, the vertical riser, and other horizontal/vertical pipe sections was performed using the Eulerian-Eulerian approach, also known as two fluids modeling, as both phases are treated as continuum and inter-penetrating continua. The solid-phase stresses are modeled using kinetic theory of granular flow (KTGF). The computed results for particle velocity were compared with the experimental data. We observed that the convection and diffusion terms in the granular temperature could not be neglected in gas-solid flow simulation along the eductor and riser pipe. The particle-wall collision and lift also play important roles in Eulerian modeling. We investigated the effect of flow parameters like gas velocity, particle properties, and particle loading on pressure drop prediction in different pipe lengths. Pressure drop increases with gas velocity and particle loading. The gas velocity has the same effect (proportional to v^2) as single-phase flow on pressure drop.

The governing PDE equations of fully developed gas-solid flow based on an Eulerian-Eulerian approach and KTGF are described as follows and were numerically solved using the COMSOL PDE solver module.

Momentum equation:

$$\rho \frac{\partial \mathbf{u}}{\partial t} + \rho (\mathbf{u} \cdot \nabla) \mathbf{u} = -\nabla p - \nabla \cdot (\rho c_s (1 - c_s) \mathbf{u}_{\text{slip}} \mathbf{u}_{\text{slip}}) + \nabla \cdot [\eta (\nabla \mathbf{u} + \nabla \mathbf{u}^T)] + \rho \mathbf{g} \quad (7)$$

$$\rho = (1 - \phi_s) \rho_f + \phi_s \rho_s \quad (8)$$

$$\eta = \eta_f \left(1 - \frac{\phi_s}{\phi_{\text{max}}} \right)^{-2,5 \phi_{\text{max}}} \quad (9)$$

Where

- \mathbf{u} Mass averaged mixture velocity
- p Pressure
- \mathbf{g} Gravity vector
- c_s Dimensionless particle mass fraction
- \mathbf{u}_{slip} Relative velocity between the solid and the gas phase

- ρ Mixture density
- ρ_f Pure-phase density of gas
- ρ_s Pure-phase density of solids
- ϕ_s Solid-phase volume fraction
- η Mixture viscosity
- η_f Dynamic viscosity of the pure-phase gas
- ϕ_{\max} Maximum packing concentration

Continuity equation:

$$(\rho_f - \rho_s)[\nabla \cdot (\phi_s (1 - c_s) \mathbf{u}_{\text{slip}})] + \rho_f(\nabla \cdot \mathbf{u}) = 0 \quad)$$

Transport equation for the solid-phase volume fraction:

$$\frac{\partial \phi_s}{\partial t} + \nabla \cdot (\phi_s \mathbf{u}_s) = 0 \quad)$$

$$\mathbf{u}_s = \mathbf{u} + (1 - c_s) \mathbf{u}_{\text{slip}} \quad)$$

Where

- \mathbf{u}_s Solid-phase velocity

Particle flux:

$$\frac{\mathbf{J}_s}{\rho_s} = -[\phi D_\phi \nabla(\dot{\gamma} \phi) + \phi^2 \dot{\gamma} D_\mu \nabla(\ln \mu)] + f_h \mathbf{u}_{\text{st}} \phi \quad)$$

$$D_\phi = 0,41a^2 \quad (14)$$

$$D_\mu = 0,62a^2 \quad (15)$$

$$\dot{\gamma} = \sqrt{\frac{1}{2}(4u_x^2 + 2(u_y + v_x)^2 + 4v_y^2)} \quad (16)$$

$$\mathbf{u}_{\text{st}} = \frac{2a^2(\rho_s - \rho_f)}{9\eta_0} \mathbf{g} \quad (17)$$

Where

- u_{st} Settling velocity of a single particle surrounded by gas fluid
- D_φ and D_μ Empirically fitted parameters
- a Particle radius
- $\dot{\gamma}$ Shear tensor magnitude

6.2.3 Model Validation on Eductor Operation

Dimensions of the commercially available eductor and attached fittings used in the experimental unit were measured and used in the transient 2D solid-gas flow model as illustrated in Figure 13. Because the particles do not flow with an even distribution across the pipe, the particle flow rate is computed by integrating the particle flow rate along the pipe diameter. Model boundary conditions (BCs) and predicted particle velocity are illustrated in Figures 13 and 14, respectively.

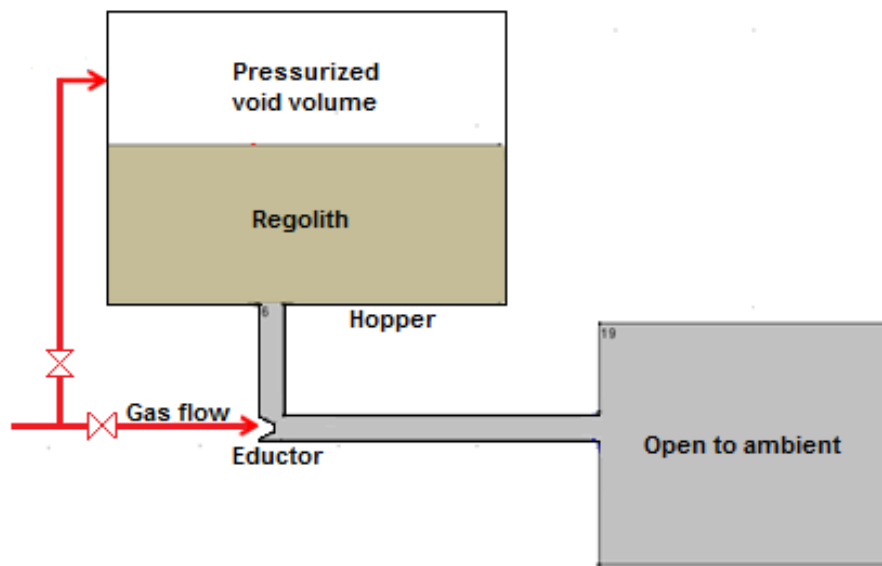


Figure 13. Eductor boundary conditions used in the model based on actual experimental setting

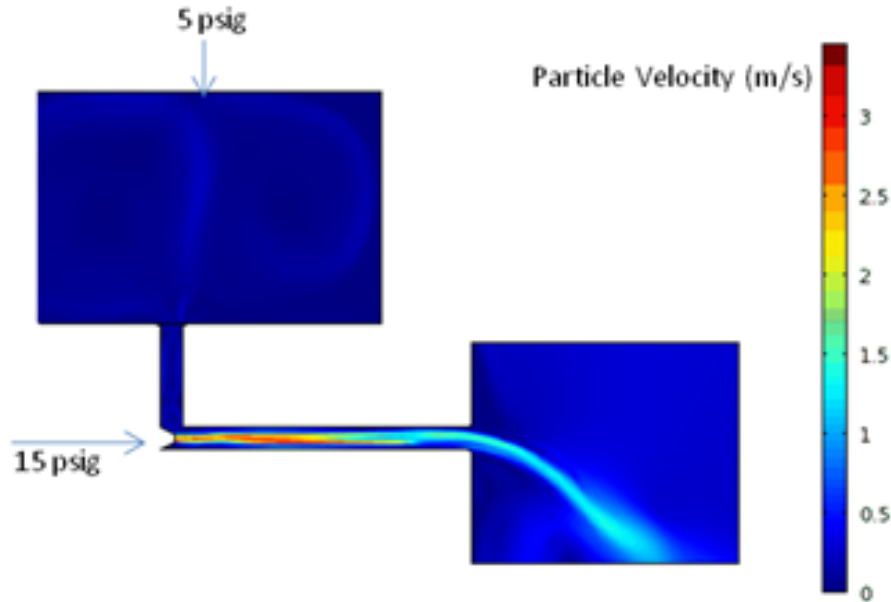


Figure 14. Particle velocity profile forecasted by the model using the BCs of Figure 13

6.2.4 Experimental Setup to Validate Model on Eductor Performance

An experimental test on the eductor was performed at the Granular Material and Regolith Operations (GMRO) laboratory at the Kennedy Space Center. Figure 15 shows images of the experimental setup used to measure the correlation of the gas pressure (or flow rate), the pressure inside the hopper, and the solid flow rate. Two pressure gauges were used to measure and record both pressures (inside the hopper and the eductor inlet probe); the entire unit was mounted on a scale to measure the transient mass loss expelled by the eductor and to estimate the regolith mass flow rate.

MODEL VALIDATION

| | |
|---------------|---------------------|
| Date: | 7, 8, 12 April 2011 |
| Material: | JSC-1A |
| Carrier Gas: | Dry Air |
| Temperature: | 22.8 C |
| Performed by: | J. Mantovani at KSC |

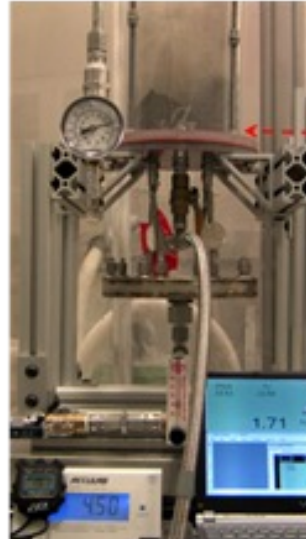


Figure 15. Experimental setup to validate model on the eductor performance

6.2.5 Model Validation Using Experimental Data

A set of experiments was conducted at the GMRO laboratory in Kennedy Space Center using air as the carrier gas. Two different pressure values (5 psig and 10 psig) at the hopper were set up to run the tests at different inlet pressures within a range of 16 psia and 45 psia (Fig. 16.)

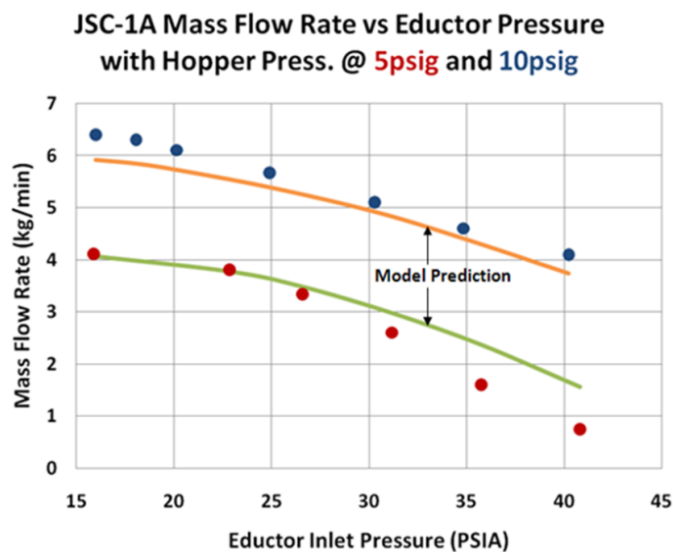


Figure 16. Experimental validation of the eductor performance model

Figure 16 shows the results along with the values predicted by the model using the conditions set in the experiment runs. As predicted by the model, the pressurization of the regolith hopper is the critical operational variable to increase solid mass flow rate as an increment of inlet pressure does not yield an increment on the mass flow rate. Solid mass flow rate was determined by measuring the system mass change with time.

6.3 Energy Sources for Conversion Applications

The delivery of energy and power required to sublimate ices and then to pressurize systems with the resulting gas dictates the types of energy sources that can be considered effectively. Radioisotopes thermoelectric generators (RTG) have a proven spaceflight heritage demonstrated by their monopoly as power sources for deep space missions where solar illumination is too dim for power conversion. However, while radioisotope sources have much higher specific energy (J/kg) than other energy sources, they offer low specific power (W/kg) but have long been used that way. According to Howe et al. (Howe, 2010), Pu-238 has a specific energy of 1.6×10^6 MJ/kg thus 160,000 times that of many chemical propellants. This translates to a system providing 4×10^5 MJ/kg of electrical energy assuming 25% conversion efficiency compared to 0.72 MJ/kg supplied by Li-ion batteries. The slow delivery of this large energy by simple decay enables the operation of onboard electrical systems at low power levels but would not be able to provide the power for sublimation systems and their applications. Howe proposed a different use of radioisotopic decay by accumulating the heat generated over long period in the form of a heat capacitor, capable of providing larger specific power for applications. The authors studied such a system to power a CO₂-based cold gas propulsion for hopper on the surface of Mars. Their work favors the adoption of a Stirling engine with flight heritage and conversion efficiencies on the order of 29% while thermoelectric systems are selected as a secondary system in their current state of the art that does not offer such efficiencies (e.g., ~7%.) The Mars Hopper concept uses a radioisotope source (Pu-238 or Am-241) encapsulated in tungsten heating a beryllium core to obtain a high temperature pressurized CO₂ tank for propulsion. A portion of the thermal power is also used to run a cryocooler that liquefies the CO₂ from the Martian atmosphere. Such a system is at first glance a suitable option to power sublimation systems that we envision and has the advantage of being operational anywhere in the solar system using gases from sublimated ices.

A comparison of the above system with photovoltaic arrays was done on the basis of the specific mass. The specific mass of the above radioisotope thermal capacitor system would approximate 2.55 kg/kWt and 8.8 kg/kWe according to the published numbers. Some of the heat is used to be converted into electrical power for the cryocooler via a closed loop Stirling engine that yields a specific power of 109 W/kg. Recent published data on advanced FAST photovoltaic arrays project a specific mass on the order of 7.5 kg/kWe (133 We/kg of specific power) at Mars around 2020 (Scott, 2013). This performance is promising for future photovoltaics as a source of energy. When power management and distribution (PMAD) and thermal cycling of the CO₂ resource are added, the numbers reach between 9 and 10 kg/kWe for a photovoltaics system, as a preliminary estimate. The radioisotope-based option can also claim longer system

longevity and reliability as a surface energy source in the Martian environment, at least on paper.

7. APPLICATION CONCEPTS OF IN-SPACE PROPULSION USING PLANETARY RESOURCES

The phase change of several compounds found across the Solar System is feasible at various energy costs. Thus the energy argument helps envision possible applications on planetary surfaces. The following applications were considered.

7.1 Cold/Warm Gas Propulsion for Hoppers

Hoppers have been envisioned for planetary surface explorations for some time (See Figure 17 for an illustration of this concept.)

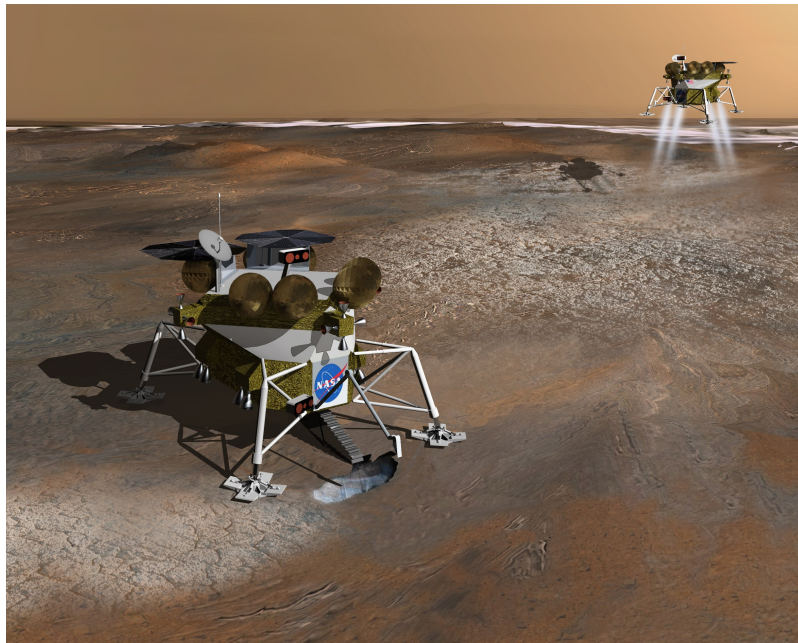


Figure 17. Small robotic exploration spacecraft collect and sublime CO₂ ice at the Martian polar cap to use in attitude-control thrusters

Image Credit: JPL (Mars landscape)/Bruce Hardman, KSC (spacecraft and overall image)

The results yielded by the propulsion model previously described show that the best candidate gases for this type of propulsion engine are those with both low molecular weight and a low critical point (P,T). Lower molecular weight compounds contribute to higher ejection velocities and larger impulse, while a low critical point allows the use of lower P,T initial tank conditions and/or longer thrust times before the gas changes phase in the tank and chokes the engine. Figure 18 shows that these facts favor gases such as oxygen, N₂, carbon monoxide (CO) and CO₂, and CH₄ that are found in planetary atmospheres or in the form of ice. Although water has a substantially larger molecular

weight, its usefulness as a cold gas propellant is mostly limited by its high critical point. This requires the pressurization of water vapor at high pressures and high temperatures to feed the thruster. Even in such cases, the change in thermodynamic conditions of the gas during expansion is so rapid that the gas velocity is reduced very rapidly and the overall thrust very limited. As shown in Figures 19 and 20, a thrust of 85 N is obtained after the starting conditions of the gas are 2,900 psia and 923 K. However condensation would occur after a mere 2 s of operation at a gas temperature of 400 K. This total thrust situation leads to very limited applications of water vapor propulsion because the pressure tanks holding the gas, the lines and valves of the system would likely be prohibitively too heavy to justify the use of such system.

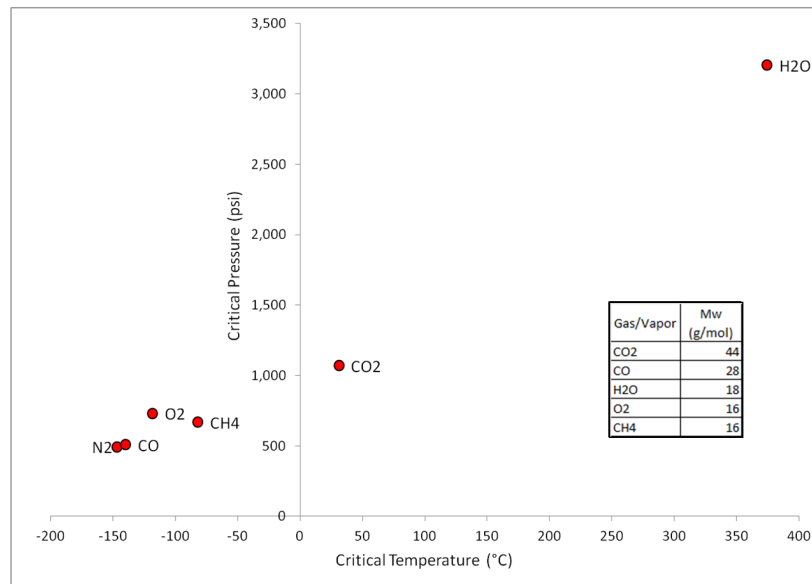


Figure 18. Critical PT (Pressure-Temperature) coordinates and molecular weight of water, CO₂, CH₄, O₂, CO, and N₂

The combination of low critical PT and lower molecular weight contribute to higher performance for cold gas propellants.

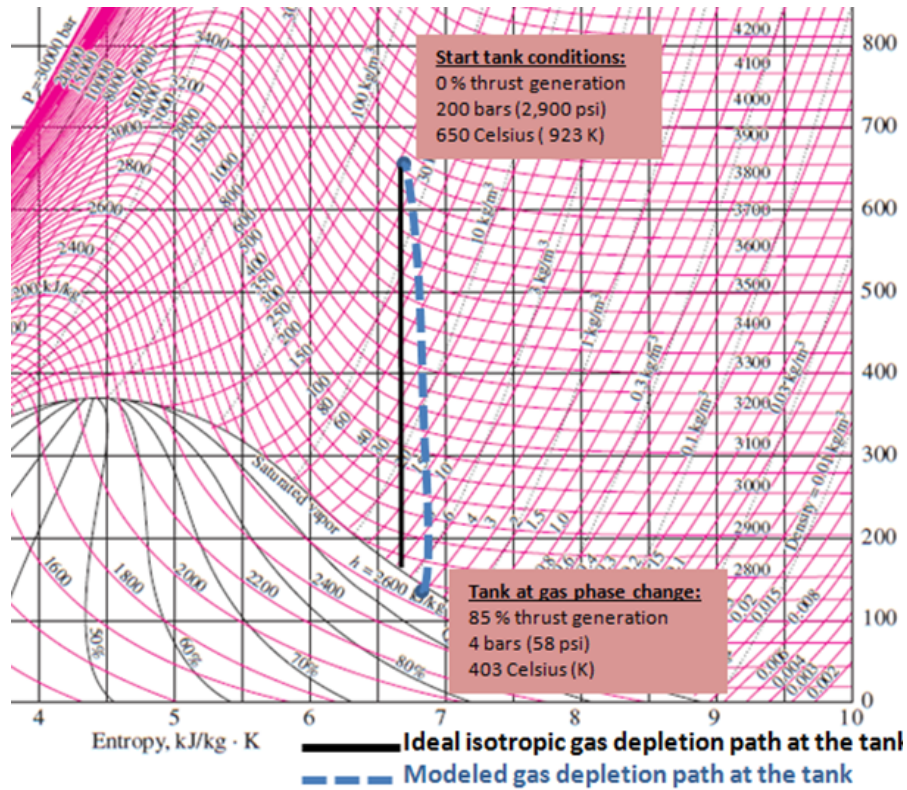


Figure 19. Modeled path conditions inside the tank originally filled with superheated water vapor at 2,900 psi and 923 K to generate thrust

The model predicts condensation of the gas inside the tank after 85% of water vapor has been depleted yielding thrust (blue dash line). The model also forecasts a deviation from ideal isotropic expansion (black continuous line).

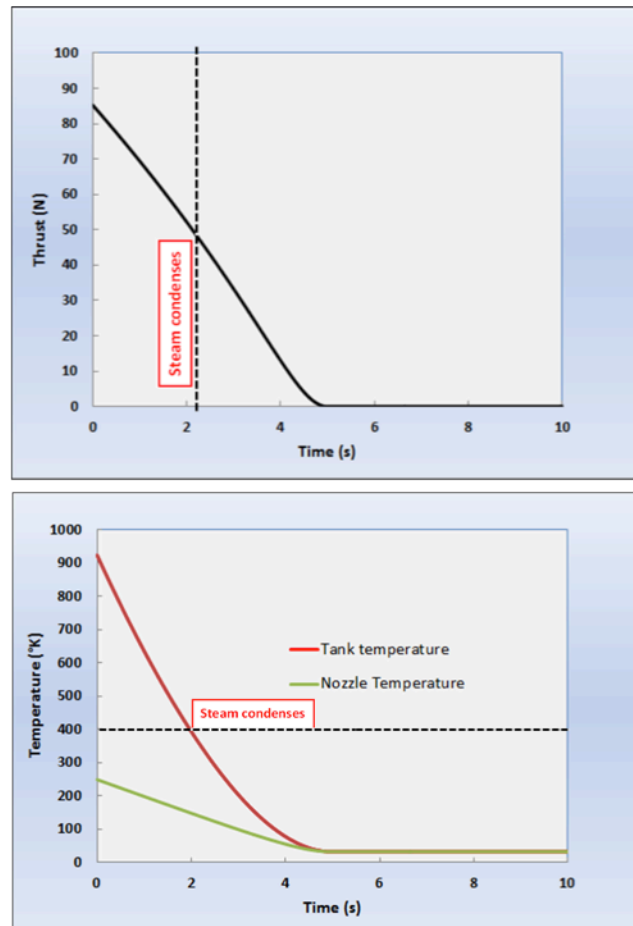


Figure 20. Modeled transient thrust and temperature profiles (at the tank throat and the nozzle) when tank is initially filled with water vapor at 2,900 psi and 923 K to generate thrust

The model predicts a thrust peak of 85 N for a 12-liter tank equipped with a 7-mm-diameter nozzle.

Using water for propulsion is problematic for two reasons: the sublimation of water requires a lot of energy (2.6–2.8 MJ/kg for pure ice; ~3.1 MJ/kg for ice in regolith) and requires pressurization of the extracted steam at high pressure and temperature values (15–20 bars; 700 °C) to generate sufficient thrust while avoiding condensation or freezing at the nozzle.

The use of CO₂ is far more feasible on Mars, for example, and presents some interesting possibilities for hoppers and other applications described below. In fact, a cold gas hopper using CO₂ obtained from the Martian atmosphere is under study by researchers and engineers at Idaho National Laboratory and the University of Leicester (Howe, 2010.) The concept increases the specific power of radioisotope energy sources by storing their decay heat and releasing it to heat up CO₂ gas rapidly to produce thrust. The atmospheric CO₂ gas is first liquefied onboard before being transferred to a thruster tank. Once initial pressure is achieved by heating, the thruster is operated. The authors

have concluded that a hopper ranging from 10 to 200 kg could achieve hopes between 10 and 30 kms every 4-5 days.

The modeled CO₂ case we present in Figures 21 and 22 shows the major difference with the case of water. Thrust can be produced for much longer times under similar thermodynamic conditions.

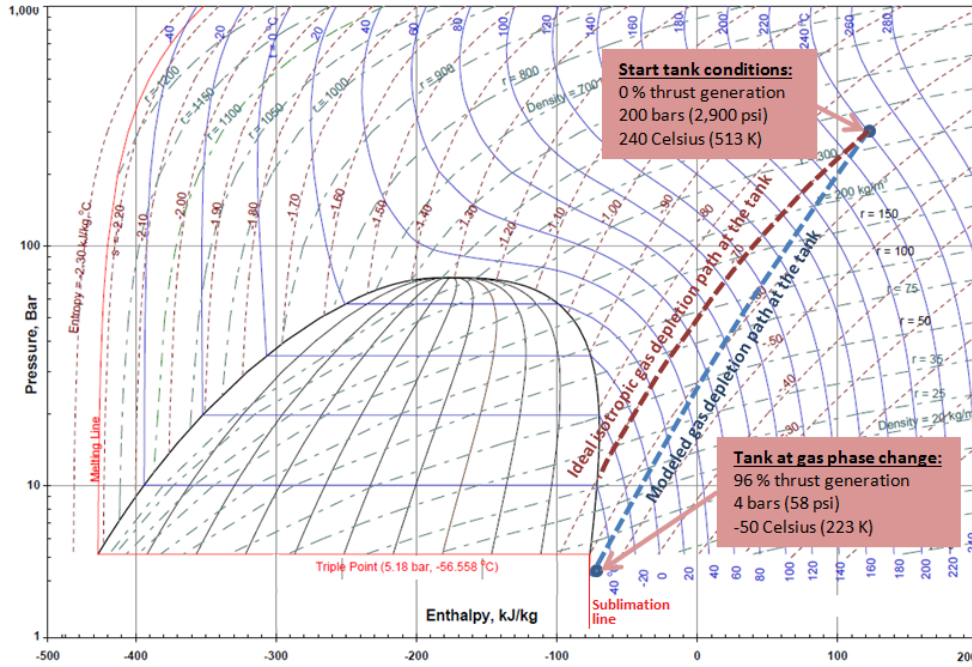


Figure 21. Modeled path conditions inside the tank originally filled with CO₂ gas at 2,900 psi and 513 K to generate thrust

Based on Figures 21 through 24, the model predicts condensation of the gas inside the tank after 96% of the gas has been depleted while generating thrust (blue dash line). The model also forecasts a deviation of ideal isotropic expansion path (red dash line). The original CO₂ chart in Figure 21 on which path lines are drawn was created with CO2TabTM and published by ChemicalLogic Corporation.

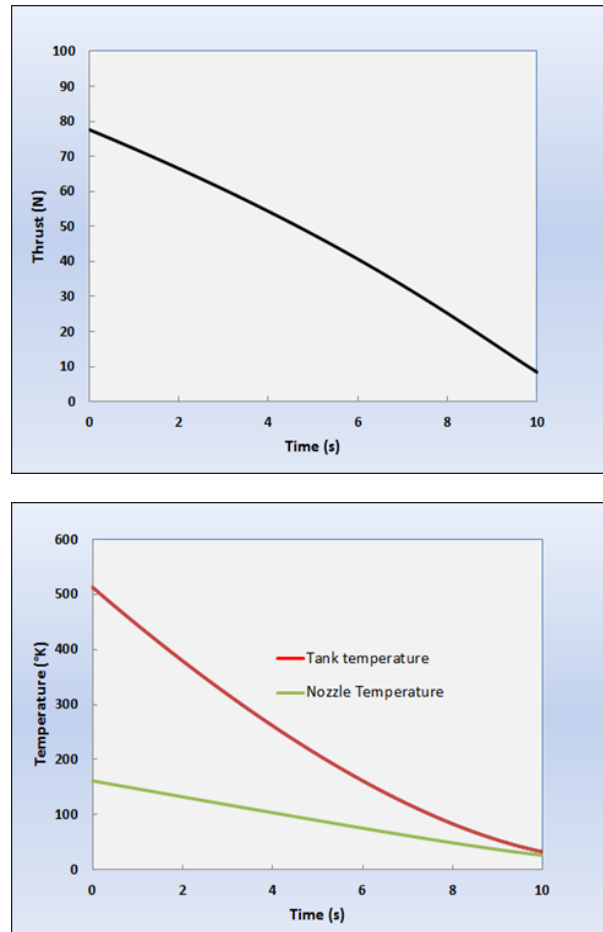


Figure 22. Modeled transient thrust and temperature (at the throat and the nozzle) profiles as the tank is originally filled with CO₂ gas at 2,900 psi and 513 K to generate thrust

The model predicts a thrust peak of 78 N for a 12-liter tank equipped with a 7-mm-diameter nozzle.

The CO₂ case yields a thrust on the same order as the one obtained with water but the engine functions until its propellant is exhausted without creating a phase change. In our modeling for low thrust values, such cold-gas engines have a lot of promise for micro-hopper robots to deploy instrumentation over large distances or to conduct exploration over long periods of time.

Using N₂ and CH₄ under the right conditions also shows promise because these gases do not require initial high tank pressures and temperatures to perform as propulsive gases while avoiding condensation. Propulsion using sublimated or vaporized CH₄ on Titan is particularly interesting because the existence of surface water ice confirmed by the

Huygens probe on the Saturnian moon creates the possibility for oxygen extraction. The possibility of CH₄ combustion to realize chemical propulsion entirely from space resources would be an exciting prospect so far from Earth.

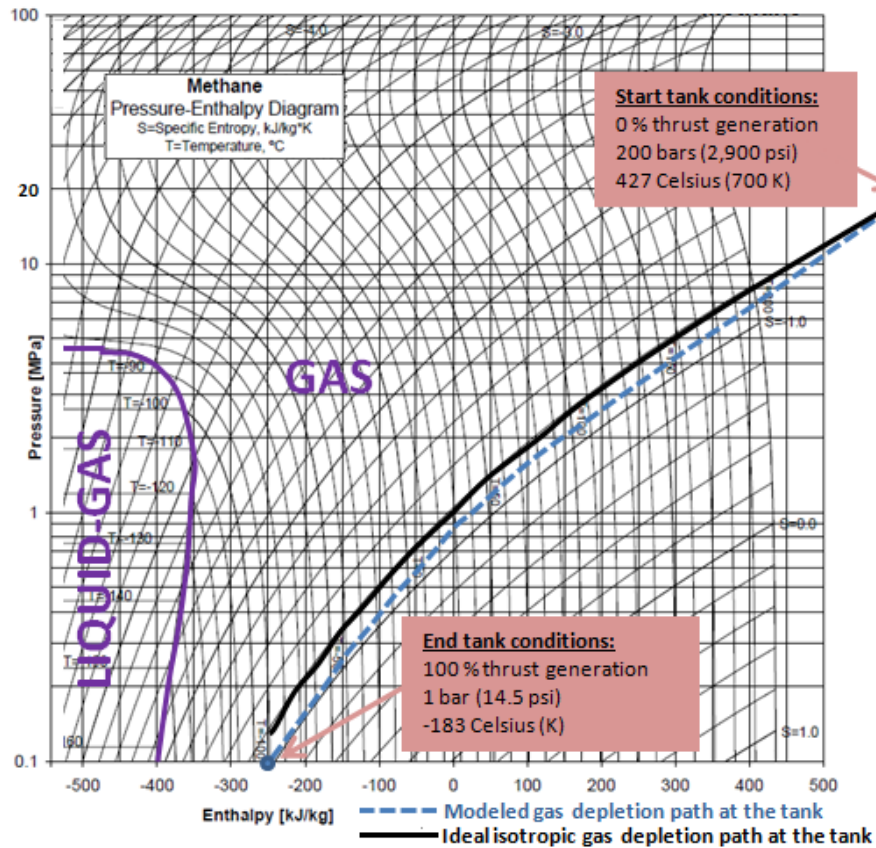


Figure 23. Modeled path conditions inside the tank originally filled with CH₄ gas at 2,900 psi and 700 K to generate thrust

The model predicts a depletion path without phase change (blue bold dash line). The model also forecasts a deviation of the ideal isotropic expansion (black bold dash line). Original methane pressure-enthalpy diagram chart produced by I. Aartun, NTNU 2002 based on the program Allprops Center for Applied Thermodynamics Studies, University of Ohio.

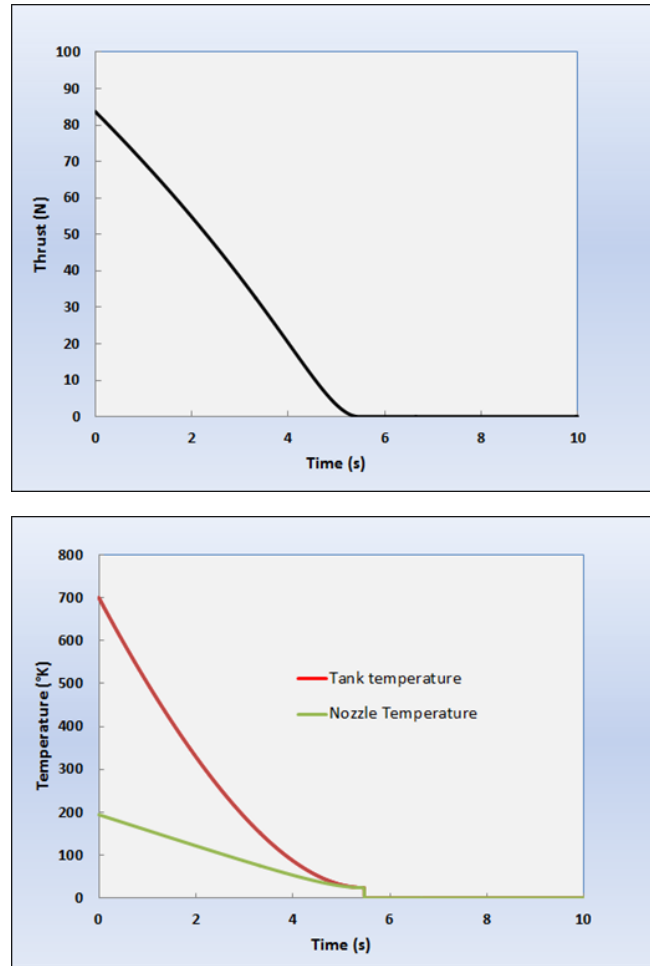


Figure 24. Modeled transient thrust and temperature (at the throat and the nozzle) profiles as the tank is originally filled with CH₄ gas at 2,900 psi and 700 K to generate thrust

The model predicts a thrust peak of 84 N for a 12-liter tank equipped with a 7-mm-diameter nozzle.

7.2 Compressed Gas Launch of Ballistic Objects

Once obtained by sublimation, the same gases under similar conditions can launch objects ballistically during surface missions. This concept of operation is envisioned to preposition surface assets, such as beacons or radio-markers, for surface navigation or landscape surveys. Instrumentation, such as seismological detectors and sample acquisition microbots, can also be sent to different locations in this way. The small compact payloads do not carry any propulsion system or propellant themselves so their mass can be kept low while focusing their design on structures that survive landings in rough terrain. A launch system can be deployed at a site rich in ice deposits where the ground support infrastructure processes the icy regolith to generate and pressurize gases. The power of the launch tubes or rails can be made variable by system design to

accommodate craft and payloads that would arrive at the site in the future to take advantage of the launch site. These small payloads may also participate in aerial surveys if the system assists the launch of aircraft. Rovers may be helped or their range of accessible targets extended by using pre-positioned system to launch harpoons across canyons or up-slope. Figure 25 displays examples of ballistic trajectories of small mass payloads using CO₂ as propellant under similar conditions as those examined previously in the model in a 1/6 g gravity field. The compressed gas launch system could also be placed onboard the ballistic craft if greater mobility is desired.

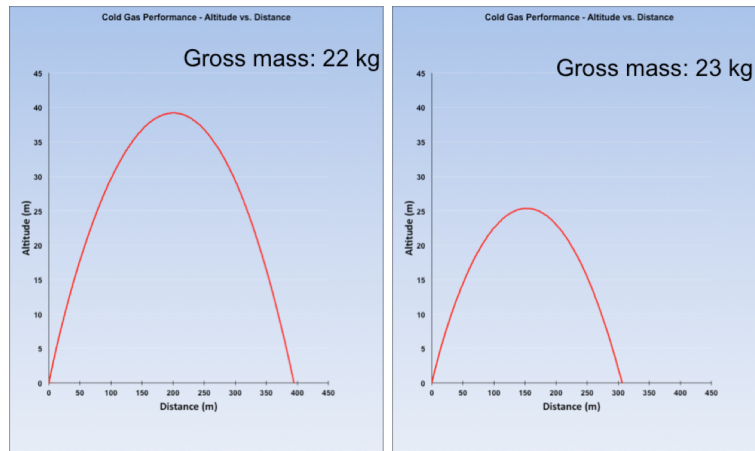


Figure 25. Small payloads ballistic trajectories in lunar gravity using CO₂ as cold gas propellant with initial tank conditions: 300 bar, 513 K, gas mass 3.2 kg. Launch angle is 60°

In the late 60's and early 70's, Howard Seifert led a team on a study of a lunar hopping transporter that uses N₂ as a propulsive cold gas in a mostly conservative cycle since most of the energy expended during launch is recovered in gas compression upon landing using the same piston (Degner, 1971.) The Pogo-like hopper was designed for fast manned transport across the lunar surface and envisioned the consumption of N₂ would be the equivalent of 4% of the system weight in N₂ for a 10 mile traverse by one crew (Meetin, 1974.) The end of the Apollo program terminated the need for greater mobility on the Moon but the concept has value for smaller robotic craft on Mars using CO₂ or Titan using N₂ and other destinations where volatile gases can be sublimated or acquired from atmospheres. Navigation, attitude control and abort systems using thrusters to alter the ballistic flight are required to avoid landings in hazards and can be embedded with much lower mass than was possible in the 70's.

7.3 Hovercraft (Surface Sublimation of Ice Sheets)

The surface of Europa is covered with water ice sheets. While rovers properly equipped with spiked wheels are a promising concept, the ice sheets also make it possible for hovercraft to traverse the terrain at higher speeds. Our knowledge of the surface to date indicate that it features vast expanses of smooth ice and temperatures ranging from -160 °C in low latitudes to -220 °C in polar regions maintains the ice as hard as granite. The weak gravity field on Europa (0.134 g) is also favorable to the hovercraft by lowering the

amount of uplift force that must be generated. In this case, energy input directly from the underside of the craft is directed at the ground surface to generate vapor under a skirt designed to create the desired pressure given the ambient conditions. Alternately, the energy can be used to generate gases for propulsion as well. The concept only appears viable when compact and relatively low-mass energy sources, such as radioisotope generators with thermal capacitors capable of rapid heat release under skirt are used. Radiant heat sources distributed below the craft would expose the icy surface underneath to rapid heating with the help of reflective flexible skirts.

Radiolysis is a dominant phenomenon in Europa's surface chemistry. Europa is subjected to intense bombardment by jovian magnetospheric particles—energetic electrons, protons, sulfur ions, and oxygen ions — that participate in the composition through radiolysis. The energetic particle's energy flux is $\Phi \approx 5 \times 10^{10} \text{ keV s}^{-1} \text{ cm}^{-2}$ creating a production rate of H_2O_2 of $\approx 2 \times 10^{11} \text{ molecules s}^{-1} \text{ cm}^{-2}$ by dissociation of H_2O molecules followed by recombination of OH radicals (Carlson, 1999). A radiolysis layer on the order of $180 \mu\text{m}$ is created in which such molecules exist. The hovercraft concept could be aided energetically by enhancing the radiolysis effects under the skirt by accelerating the energetic particle flux from Jupiter using spaced alternating electrodes and channeling it by electrostatic and electromagnetic lenses akin to a transmission electron microscope. The continuous production of these specie at high rate would then create a layer that can be heated at a reduced overall energy cost to generate the required pressure and gas flow. The concept would be applicable on the satellites of the ice giants Uranus and Neptune where the particle flux are accelerated in a strong magnetosphere.

The hovercraft concept can find application on Titan's surface as well, largely covered by thick ice sheets and peppered by hundreds of methane lakes; the hovercraft then edges out the rover by extending mobility over both ice and liquid. However, a hovercraft operating on Titan would not sublimate the ice or vaporize the liquid underneath it; instead it would more likely blow the dense $\text{N}_2\text{-CH}_4$ gas around it downward into the skirt like an terrestrial hovercraft. Recently, such hovercraft was among options considered by researchers proposing the TALISE mission to explore the lakes on Titan that ultimately favored the use of a boat propelled by wheel or screw (Urdampilleta, 2012.)

7.4 Pneumatic Regolith Transfer Using Low Pressure CO_2

Based on the solid-gas flow model described previously and validated experimentally in the eductor stand-alone operation in the GMRO laboratory (Figs. 13 and 14), we modified the boundary conditions in the model to include gas inlet feeders into the hopper to represent accurately the fluidization of the regolith bed at its base. We then conducted a study on pneumatic transportation of the same granulated material but using CO_2 gas in an open system. The model includes horizontal and vertical/riser pipe sections that can feed material to a processing reactor via an additional hopper as well as the cyclone between the eductor and the reactor to model all the units needed to pneumatically transport granulated material. The model results describe the use of CO_2 gas in an open system, with a discharge pressure (the open end of the riser) at 500 torr.

Figure 26 illustrates the gas phase velocity profile in steady-state mode and shows that the gas is fed to both the eductor and the hopper. The model's boundary conditions include the inlet pressure and velocity at the inlet of the nozzles connected to the hopper and the eductor. Pressure at the end of the riser pipe is also a boundary condition.

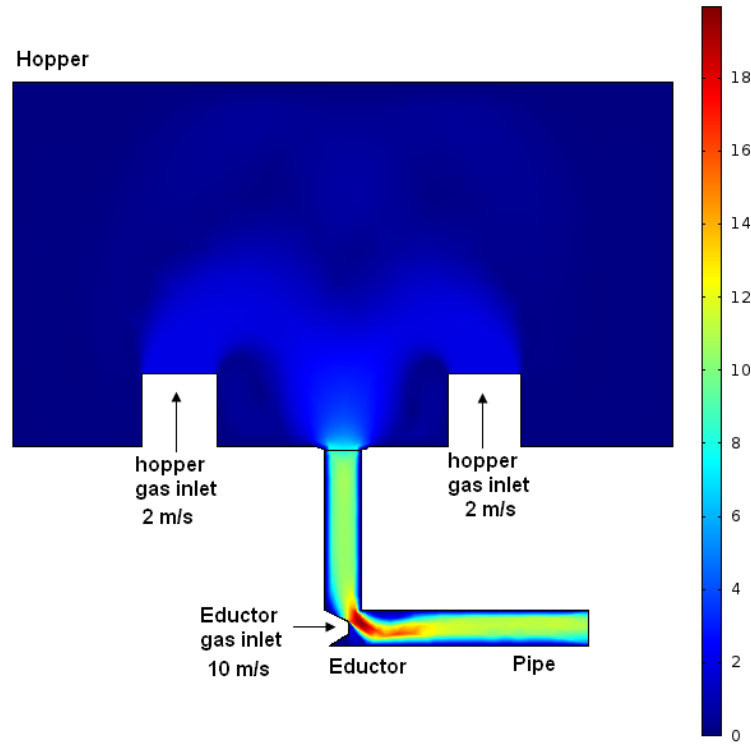


Figure 25. CO₂ gas velocity profile modeled using two nozzles with the area equal to the total area of small nozzles actually in place inside the hopper

Boundary conditions include inlet velocity/pressure at the nozzles and the eductor as well as the pressure at the outlet of the pipe.

Figure 27 illustrates the solid/granulated profile of the gas phase in transient mode before reaching temporary steady-state mode. The model was run to estimate granulated flow rate at different inlet pressures for a given riser length. As predicted and validated above,

for a given hopper pressure and riser length, the maximum granulated/solid flow rate is achieved as the eductor inlet pressure gets close to the hopper's pressure.

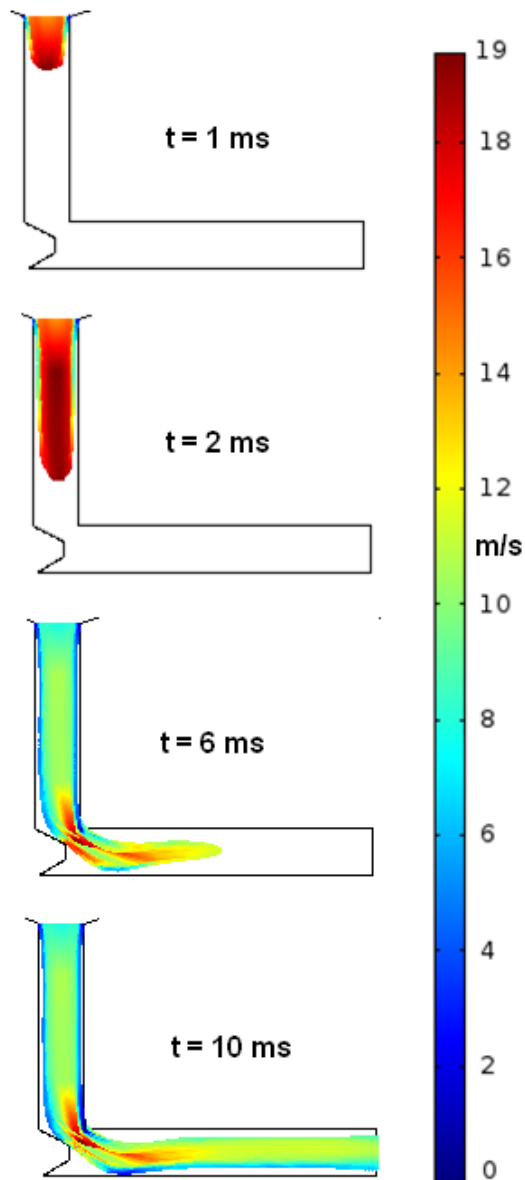


Figure 26. Transient particle (solid phase) velocity profile modeled using the gas flow conditions of Figure 24

Figure 28 shows the results of modeling the pneumatic transportation of granulated material with a diameter of 2.5 mm using CO₂ gas that could come from sublimated Martian CO₂ ice. The model predicts maximum mass flow rate of solid material on the order of 3 kg/min to 6.5 kg/min when pressures at the eductor are slightly above those at the hopper containing the starting material. These flow rates decrease as expected when one attempts to convey the regolith at higher heights set by the riser from 0 m to 2 m. Extrapolating the results to 5 psia as hopper and eductor inlet pressures with no riser leads to a rough estimate of 1.6 kg/min of regolith flow. A molecular flow approach

would be needed to model discharge flow from high pressure to vacuum (Mars and asteroid ambient). It is clear that low CO₂ pressures can be used very effectively to perform transport of regolith, and while our current tools did not allow us to model transport at less than 500 torr, we believe that significant and promising work will demonstrate the use of even lower pressures.

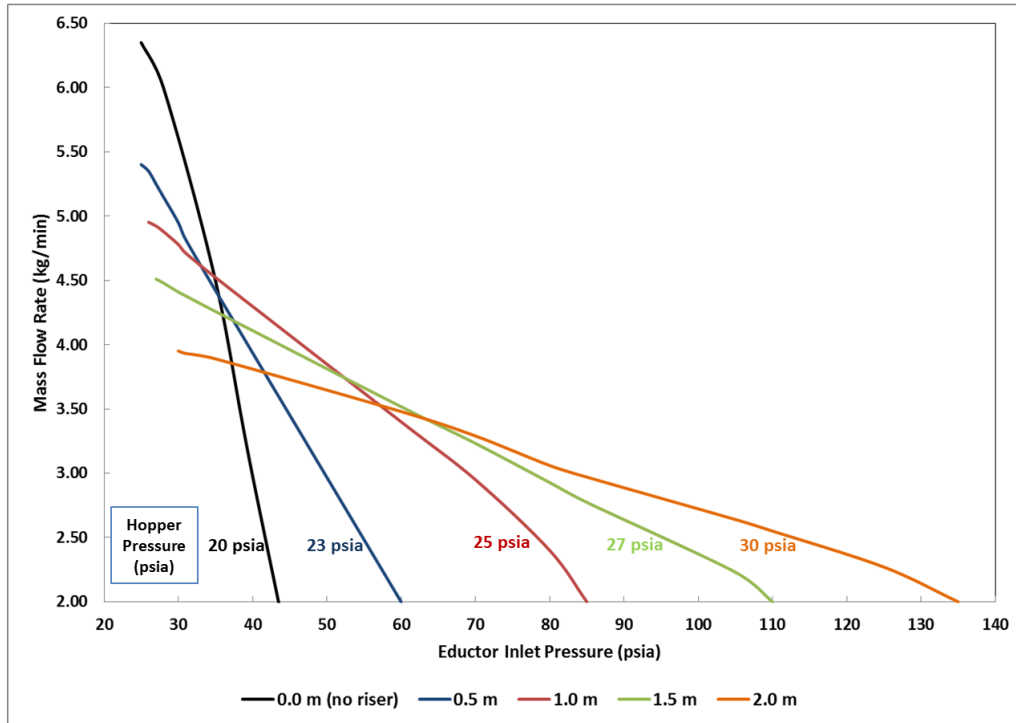


Figure 27. Solid mass flow rates predicted for various eductor/hopper pressures to convey regolith at different heights

8. SPECIAL APPLICATION: ASTEROID AND COMET DEFLECTION BY EJECTION OF *IN SITU* VOLATILES

The ejection of volatile materials contained in asteroids and comets was examined to assess the potential of deflecting these threatening objects from a collision path with Earth. While deflecting dry rocky or metal asteroids would require a reactor capable of volatilizing oxides or metals at high energy costs (as treated previously) or a system designed to mine and eject regolith and rocks as treated by Olds and co-workers (Olds, 2007,) we believe that the sublimation of various ices in comets and icy asteroids holds promise. Figure 29 shows the projected masses that must be ejected from a 400 m diameter asteroid/comet to change its orbital parameter by a Δv of 0.1m/s. This change in orbital velocity is in agreement with target values for a deflection on the order of one Earth radius in an analysis of deflection scenarii for Earth-crossing asteroids by Park and Mazanek (Park, 2005.) It gives an order of magnitude of what is required given the amount of time available: this deflection is feasible if ~25 kg of material can be ejected

per second continuously for 100 days. If the time afforded to the deflection mission is a year, the ejection rate drops to 7 kg/s.

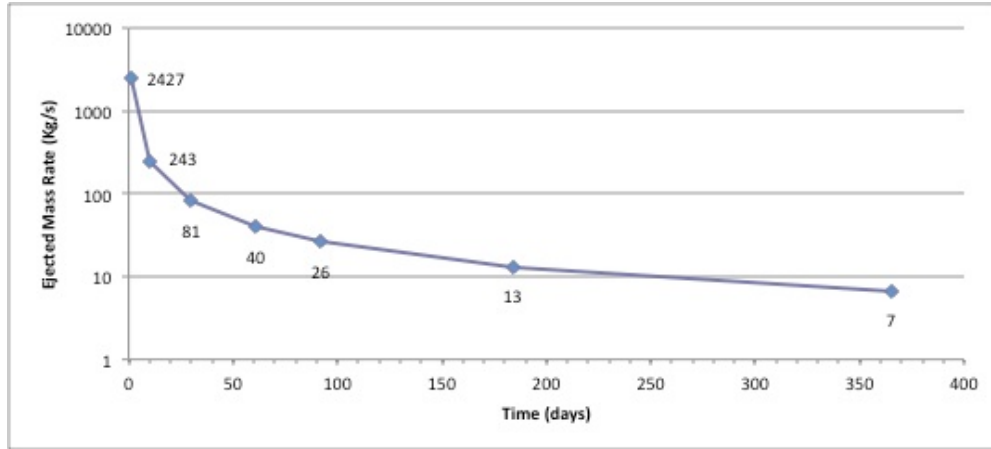


Figure 28. Ejected mass flow rate from a comet or asteroid to propel it on a deflected orbit with a Δv of 0.1m/s

Example assumes a gas/solid material velocity of 3 m/s, and an object of 400 m in diameter with a density of 2 g/cm³.

In comparison, the comet Wirtanen ejects 7.5 kg/s of gas at peak activity and temperature near the perihelion. Energetically, the reactor would have to sublime water at ~2.8 MJ/kg, but comets do contain many other volatile species—CO, CH₄, hydrogen cyanide (HCN), and NH₃—whose sublimation energies range from 0.2 MJ/kg to 1.7 MJ/kg. Furthermore, comets are thought to be reservoirs of amorphous ice, the formation of which is possible below 120K at fast condensation rates (Kouchi, 1994) and the phase transition of pure amorphous ice to crystalline ice is exothermic on the order of 1.6 kJ/mol (0.089 MJ/kg). This phase transition is a possible cause of large bursts of ejected gases in comets, even when they are far from their perihelion and where they receive little energy from the Sun (Huebner, 2006.) We propose that it may be possible to trigger the transition from amorphous to crystalline ice by a thermal trigger at depth through the implacement of a subsurface expeller tube with heaters into mixed layers of rocks and ice; additional thermal inputs bridging the value of the exothermic reaction and that of the sublimation of surrounding trapped volatile compounds would result in the evolution of gases that the expeller tubes would channel to the surface by pressure differential. The idea behind the concept is to generate a thermal event at depth that results in large amounts of propelled gas at a lower energetic cost than a 3 MW reactor would produce by sublimation of water ice only.

Such a system could cause deflection at specific points of orbit and create directed jets that would gain a fraction of a degree of deflection. We must also acknowledge several major limiting factors to such a scheme. The presence of amorphous ice is still speculative in comets although the comet simulation experiments (KOSI) carried out in large vacuum chamber at the German DLR in the 1990's lay validity to the phenomenon (Seidensticker, 1992.) The presence of impurities, either mineral or other volatile

compounds in the amorphous ice also alters the energetics of the phase transition to the point of even reversing it to an endothermic reaction in some conditions. Much remains unknown and speculative in our cumulative knowledge of the subsurface of comets and icy asteroids. Comets are also very unstable rotational objects adding tremendous complexity to a deflection scheme that include timing of a surface propulsion system. The concept illustrated in Figure 30 would likely involve multiple spacecraft positioned and repositioned on the object's surface to maximize gas production using data inputs from other sensing craft co-flying with the comet to assess its evolution and direct the timing of propulsion events. Precise observational information would be critical to the enterprise: for example, surface valleys when concave exhibit jet-like gaseification and could be features of choice. Another criterion of placement could be the presence of a dust mantle that typically reduces the activity in that area and could act as a containment dome to help channel the produced gases once perforated by the lander's drilling devices.

The porous nature of comet nuclei and many asteroids is also an opportunity to be exploited as it could enable the creation of a catastrophic rapid expansion of trapped gases if enough energy is input at depth below the surface to cause fragmentation of the entire object. The degree of control of the characteristics of the resulting objects naturally would be low. However, it may aid another planetary defense concept that merits further study; instead of trying to move the comet or asteroid off its current orbit, less energy could be expended to spin it faster and faster by increasing its initial rotational momentum until it fragments. Asymmetric spinning may also contribute to the end goal of causing breakage without trying to control the target. After examination of the remaining fragments, it would be possible to select only a few that still pose a threat that can be mitigated possibly with less energy and better success than any attempt at moving the entire body in the first place. The centrifugal motion of the ejected fragments would likely result in a cluster of small objects with parallel orbits. Some will be small enough to be classified as non-threatening to Earth even if still on a collision path with our planet while others will need to be either deflected or destroyed. In any case, their smaller size will make them easier targets. In addition, some fragments may be placed on a non-threatening course depending on the conditions of the breakage.

When the target asteroid is found to contain no ice compounds and consists of only dry mineral materials, we consider two options to perform ISRU-based propulsion of the asteroid; 1) direct laser ablation as treated above in Section 5.2 and 2) oxygen ion propulsion. Oxygen may represent about 40%–50% by weight of mineral oxides found in large asteroid populations such as S-type characterized to date, which makes oxygen decomposed from the mineral oxides an attractive choice for *in situ* propulsion. The decomposition can be performed either by melting of a pool of mineral material under the vacuum environment by laser heating or by direct oxide electrolysis of such pool. The volatile specie thus produced (Fig. 5) move rapidly to recombine with oxygen ions at these temperatures and would accordingly alter the thrust characteristics obtained by accelerating those ions. The recombination of the gas components with the hot oxygen into oxides can be mitigated by separating the oxygen from the gas stream using O₂-permeable YSZ membranes that operate best at high temperatures. The resulting oxygen gas can then be accumulated and pressurized and used as either in cold-gas or

monopropellant propulsion system or as an oxidizer for a bipropellant system. A reactor using this concept could be considered as a means to propel a rocky asteroid devoid of water, either to station the asteroid in a specific location for mining or to deflect it off a collision path with the Earth.

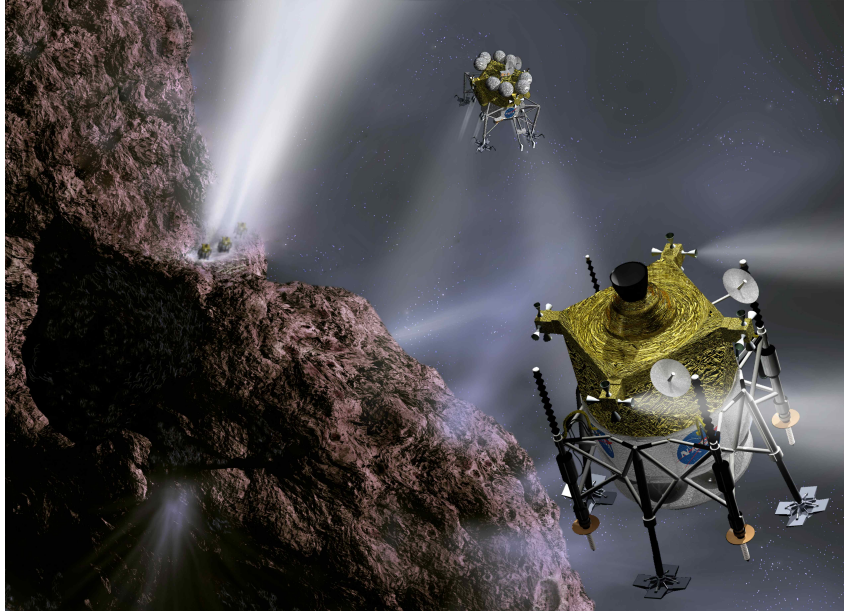


Figure 29. Conceptual mission to deflect a comet by using *in situ* propulsion

Robotic spacecraft approach the comet and anchor themselves into the surface, where they drill and collect icy material. The ice is sublimated and ejected through an on-board propulsive chamber. Image credit: JPL (Comet)/Bruce Hardman, KSC (spacecraft and overall image)

9. CONCLUSION

This project, sponsored by the NASA Innovative Advanced Concepts program, examines how the systematic use of space resources such as frozen volatiles can create a new paradigm in surface power generation for deep space missions. The ubiquitous presence of ices of water, carbon dioxide, methane, and other compounds throughout the Solar System under conditions favorable for their sublimation will enable novel in-space propulsion and actuation concepts to become a reality and to address one of NASA's Grand Challenges, "All Access Mobility." Accessing such a resource in the far corners of our interplanetary neighborhood enables us to conceive exploration missions with spacecraft that are capable of refueling in the Jovian and Saturnian systems and able to achieve new goals or reach new destinations.

This preliminary feasibility study shows that the thermodynamics limitations point to the use of ice as a gas resource for very low mass exploration robots, made feasible by emerging technologies. The low specific impulses typical of gases used in cold/warm pressure gas propulsion favor such propulsion for herds of microhopper robots weighing a few kilograms each. On Mars, using CO₂ ice for propulsion would certainly be limited

to such small craft, although the atmosphere is a much larger source of the gas and is better suited for larger hoppers. Similarly, the use of *in situ*-generated gases in pneumatic systems is feasible in many planetary locations to lift masses of a few kilograms or launch them in low-gravity fields for either successive hops or to deploy distributed networks of surface equipment. As ISRU systems are developed to process mineral resources, excavating consolidated surface material and transporting it into a reactor is shown to be feasible at high efficiencies under low gas pressure. Another method, using CO₂ gas under Martian surface conditions, was examined and showed that flow rates of regolith of several kg/min can be achieved with gas at less than 5 psia.

The extension of the concept to using other ices such CH₄, or CO in the farthest regions of the Solar System remains feasible and actually would be even more valuable even for modest performance because of the exacerbated needs for mission survival and reliability. The need to transform and use such resources in this realm to sustain missions where solar power is not an option calls for technologies capable of harnessing local energy sources. We advance such notional concept of channeling high energy particle fluxes that define the Jovian environment for example to achieve radiolysis of ice compounds. The thus-generated and collected ions could refuel ion engines propelling small probes then able to go from one moon to another and/or bring up samples to a larger orbiter in the planetary system that would perform and broadcast results of in-depth sample analysis that is not possible on the surface microbots. The low gravity fields may allow launch to orbit using ion engines.

The ice utilization concept also was found to apply to *in situ* propulsion for deflecting the orbit of a comet or an asteroid slightly in order to prevent it from colliding with Earth. Although it is very challenging to deploy adequate energy sources (one to several megawatts) on such objects, the sublimation of a series of *in situ* volatile compounds would be adequate to generate enough thrust to impart small changes in orbital velocities to objects with diameters in the few hundreds of meters. Such a strategy possibly coupled with directed fragmentation could be applied to volatile-rich objects whose threatening path to Earth is discovered years before the potential impact.

10. ACKNOWLEDGEMENTS

The authors wish to acknowledge the NASA Innovative Advanced Concepts (NIAC) program for bestowing a Phase I award to support this work and the NASA Kennedy Space Center Space Technology Office for providing encouragements and institutional support. We are also very grateful to Bruce Hardman (Kennedy Space Center) for his advice on spacecraft concept engineering and his artistic creations of our concepts.

11. REFERENCES

Ahrens, T.J. and Harris, A.W. (1992). "Deflection and Fragmentation of near-Earth asteroids," *Nature*, 360, 429-433.

Andreas, E.L. (2007). "New estimates for the sublimation rate for ice on the Moon," *Icarus*, 186, 24-30.

- Arvidson, R.E., et al. (2009). "Results from the Mars Phoenix Lander Robotic Arm experiment," *J. Geophys. Res.*, 114 (E02).
- Blackburn, D.G., Bryson, K.L., Chevrier, V.F., Roe, L.A., and White, K.F. (2010). "Sublimation kinetics of CO₂ ice on Mars," *Planetary and Space Science* 58, 780-791.
- Brown, C. D., *Spacecraft Propulsion*, American Institute of Aeronautics and Astronautics, Washington D.C., 1996.
- Carlson, R.W., et al. (1999). "Hydrogen Peroxide on the Surface of Europa," *Science* 283, 2062-2064.
- Colaprete, A., Schultz, P., Heldmann, J., Wooden, D., Shirley, M., Ennico, K., Hermalyn, B., Marshall, W., Ricco, A., Elphic, R. C., Goldstein, D., Summy, D., Bart, G. D., Asphaug, E., Korycansky, D., Landis, D., and Sollitt, L. (2010). "Detection of Water in the LCROSS Ejecta Plume," *Science* 330 (6003), 463-468 (22 October 2010).
- Coustenis, A. and Taylor, F.W. (2008). *Titan: Exploring an Earthlike World*, World Scientific Publishing, Singapore, p. 130.
- Cruikshank, D.P., Brown, R.H., Calvin, W.M., Roush, T.L., and Bartholomew, M.J., "Ices on the satellites of Jupiter, Saturn, and Uranus," in *Solar System Ices*, (1998) Eds. B. Schmidt, C. de Bergh, and M. Festou, pp. 579-606, Kluwer Acad. Norwell, MA.
- Dalton, J.B., Cruikshank, D.P., Stephan, K., McCord T.B., Coustenis A., Carlson R. W., and Coradini A. (2010). "Chemical Composition of Icy Satellite Surfaces," *Space Sci. Rev.* 153, 113-154.
- Degner, R., Kaplan, M., Manning, J., Meetin, R., Pasternack, S., Peterson, S., and Seifert, H. (1971). "The Lunar Hopping Transporter," Final Report for NASA Grant NGR 05-020-258, Stanford University, July 1971.
- Demidov, N.E., Boynton, W.V., Gilichinsky, D.A., Zuber, M., Kozyrev, A.S., Litvak, M.L., Mitrofanov, I.G., Sanin, A.B., Saunders, R.S., and Smith, D.E. (2011). "Water distribution in Martian permafrost regions from joint analysis of HEND (Mars Odyssey) and MOLA (Mars Global Surveyor) data," *Astronomy Letters* 34 (10), 713-723.
- ESA News (2005). "Seeing, touching and smelling the extraordinarily Earth-like world of Titan," *ESA News*, European Space Agency, January 21, 2005.
http://www.esa.int/SPECIALS/Cassini-Huygens/SEMHB881Y3E_0.html.
(Retrieved March 28, 2005).

- Feistel, R. and Wagner, W. (2007). "Sublimation pressure and sublimation enthalpy of H₂O ice Ih between 0 and 273.16 K," *Geochimica et Cosmochimica Acta*, 71(1), pp.36-45.
- Frank, A., Clusius, K. (1937). "The entropy of methane," *Z. Physik. Chem.* B36, 291-300.
- Gibbings A., Vasile M., Watson I., Hopkins J-M., and Burns D. (2012). "Experimental Analysis of Laser Ablated Plumes for Asteroid Deflection and Exploitation," *Acta Astronautica* 90, 85-97.
- Howe, S.D. et al. (2010). "The Mars Hopper: An Impulse Driven, Long Range, Long-Lived Mobile Platform Utilizing In-Situ Martian Resources," *Proceedings of the International Astronautical Congress*.
- Huebner, W.F., Benkhoff, Capria, M-T., Coradini, A., De Sanctis, C., Orosei, R. and Prialnik, D. (2006). *Heat and Gas Diffusion in Comet Nuclei*, ISSI Scientific Report SR-004, Ed, International Space Science Institute.
- Kouchi, A., Yamamoto, T., Kozasa, T., Kuroda, T., and Greenberg, J.M. (1994). "Conditions for condensation and preservation of amorphous ice and crystallinity of astrophysical ices," *Astron. Astrophys.* 290, 1009-1018.
- Knight, C.J. (1979). "Theoretical Modeling of Rapid Surface Vaporization with Back Pressure," *AIAA Journal* 17 (5), 519-523.
- Kuskov, O.L. and Kronrod, V.A. (2005). "Internal structure of Europa and Callisto," *Icarus*, 177 (2).
- Levison, H.F., Bottke, W.F., Gounelle, M., Morbidelli, A., Nesvorný, D. and Tsiganis, K. (2009). "Contamination of the asteroid belt by primordial trans-Neptunian objects," *Nature* 460 (16 July 2009), 364-366.
- Mars Facts (2012) <http://quest.nasa.gov/aero/planetary/mars.html>
- Meetin, R.J., and Seifert, H.S. (1974). "Propulsion dynamics of lunar hoppers," *J. Spacecraft* 11 (12), 852-856.
- Melosh, H.J., Nemchinov, I.V. and Zetzer, Y.I., "Non-nuclear strategies for deflecting comets and asteroids," in *Hazard due to comets and asteroids*, (1994) Ed. Gehrels, T., pp. 1111-1132, University of Arizona Press.
- Mohan, S., Saenz-Otero, A., Nolet, S., Miller, D.W., and Sell, S. (2009). "SPHERES flight operation, testing and execution," *Acta Astronautica* 65 (7-8), 1121-1132.
- Mungas, G., Rapp, D., Easter, R., Johnson, K., and Wilson, T. (2006) "Sublimation Extraction of Mars H₂O for Future In-Situ Resource Utilization," *Earth & Space* 2006: pp. 1-8.

- NASA (2007). *Near-earth object survey and deflection: analysis of alternatives*, <http://www.nasa.gov/pdf/171331main_NEO_report_march07.pdf>, NASA Report to Congress, <http://neo.jpl.nasa.gov/neo/report2007.html> (March 2007)
- National Research Council (2010). *Defending Planet Earth: Near-Earth Object Surveys and Hazard Mitigation Strategies*, National Academy of Sciences, Washington, D.C.
- Niemann, H.B. et al. (2005). “The abundances of constituents of Titan’s atmosphere from the GCMS instrument on the Huygens probe,” *Nature* 438 (8 Dec. 2005), 779-784.
- Olds, J.R., Charania, A.C., and Schaffer, M.G. (2007). “Multiple Mass Drivers as an Option for Asteroid Deflection Missions,” AIAA-2007-S3-7, 2007 Planetary Defense Conference, Washington, D.C., March 5-8, 2007.
- Park, S.-Y., and Mazanek, D.D. (2005). “Deflection of Earth-crossing asteroids/comets using rendezvous spacecraft and laser ablation,” *J. Astronautical Sciences* 53 (1), 21-37.
- Phipps, C.R. (1997). “Laser deflection of near-earth asteroids and comet nuclei,” *Proceedings of International Conference on Lasers 96*, pp. 580-587, STS Press.
- Rice, E.E. (2000). “Development of Lunar Ice/Hydrogen Recovery System Architecture,” NIAC Phase I Report, NASA/NIAC Research Grant 07600-021.
- Rivkin, A.S. et al. (2010). *The Case for Ceres: Report to the Planetary Science Decadal Survey Committee*, http://www.lpi.usra.edu/decadal/sbag/topical_wp/AndrewSRivkin-ceres.pdf.
- Scott, J.H., George, J.A., and Tarditi, A.G. (2013). “Direct Energy Conversion for Low Specific Mass In-Space Power and Propulsion,” in *Proceedings of Nuclear and Emerging Technologies for Space 2013*, Paper# 6756, Albuquerque, NM, February 25-28, 2013.
- Seidensticker, K.J., and Kochan, H. (1992). “Gas dynamics of sublimating ice/dust samples,” *BAAS* 24, 1019.
- Showman, A.P. and Malhotra, R. (1999). “The Galilean Satellites,” *Science* 286 (5437), 77-84.
- Stull, D.R. (1947). “Organic compounds,” *Ind. Eng. Chem.* 39, 517.
- Urdampilleta, I. et al. (2012). “TALISE: Titan Lake In-situ Sampling Propelled Explorer,” *EPSC Abstracts* 7, No. EPSC2012-64 2012, European Planetary Science Congress 2012.

Vasile M., and Maddock C. (2010). "On the deflection of asteroids with mirrors, *Celestial Mech. Dyn. Astron.* 107, 265-284.

Zacny, K., and Bar-Cohen, Y. (2009). "Drilling and Excavation for Construction and In Situ Resource Utilization," in *Mars: prospective energy and material resources*, (2009) Ed. Badescu, V., Ch. 15, Springer Science & Business Media.

Zacny, K. et al. (2009). "Extraterrestrial Drilling and Excavation," in *Drilling in extreme environments: penetration and sampling on Earth and other planets*, (2009) Eds. Bar-Cohen, Y. and Zacny, K., Ch. 6, p. 444, John Wiley & Sons.

Zubrin, R. (2000). "Section: Titan," in *Entering Space: Creating a Spacefaring Civilization*, Tarcher/Putnam, 163-166.

Appendix A. PHASE CONDITIONS OF WATER IN THE SOLAR SYSTEM

Conditions That Support the Presence of Ice Water on the Surface of the Moon, Mars, Comets, Europa, and Titan

A.1 Water Equilibrium Phase Diagram

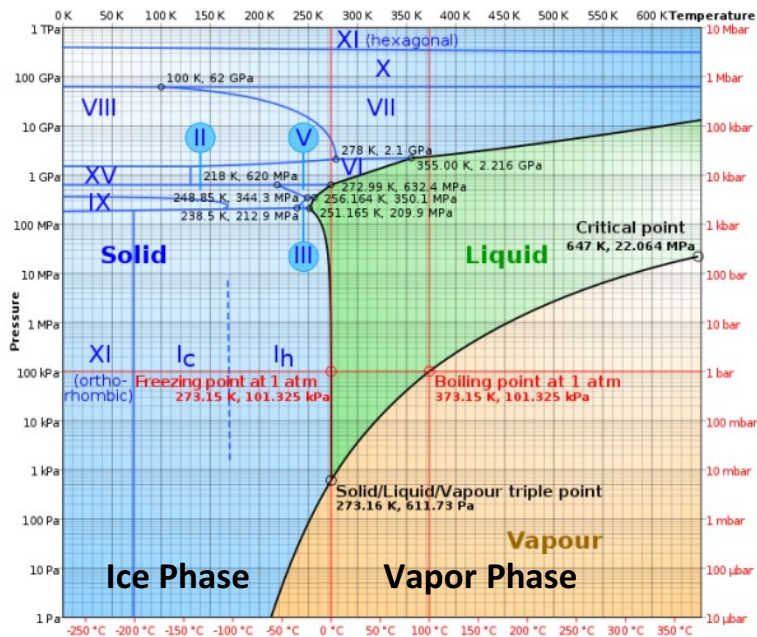


Figure 30. Water phase equilibrium at moderate pressure [1]

The Roman numerals indicate various ice phases.

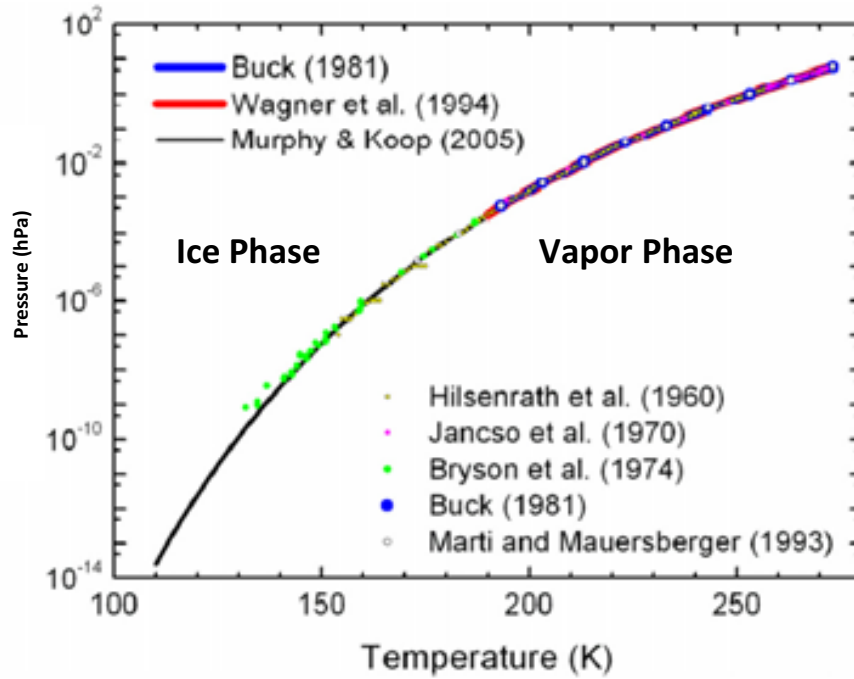


Figure 31. Water solid-vapor phase equilibrium (including vacuum conditions) measured by various researchers [2]

A.2 Moon Surface

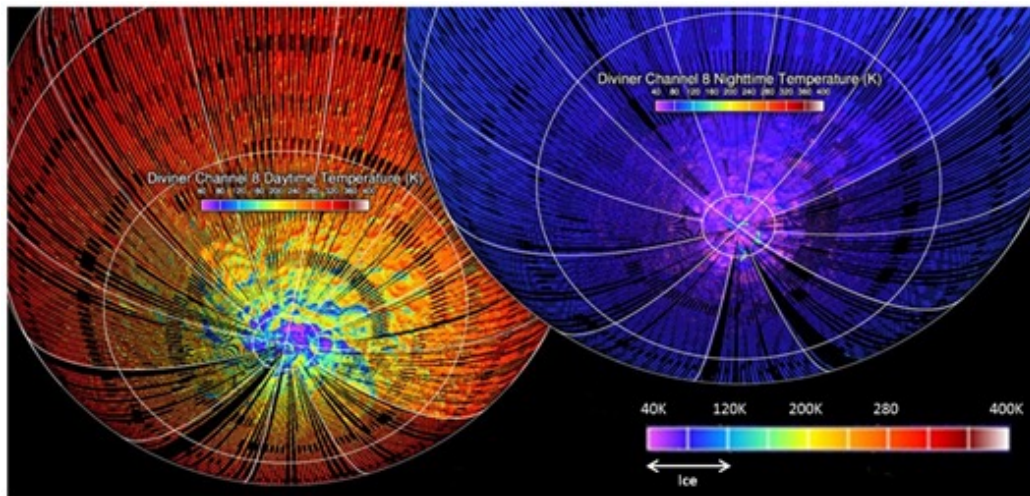


Figure 32. Daytime and nighttime temperature observations of the lunar south pole recorded by the Diviner Radiometer Experiment, one of seven instruments on NASA's Lunar Reconnaissance Orbiter

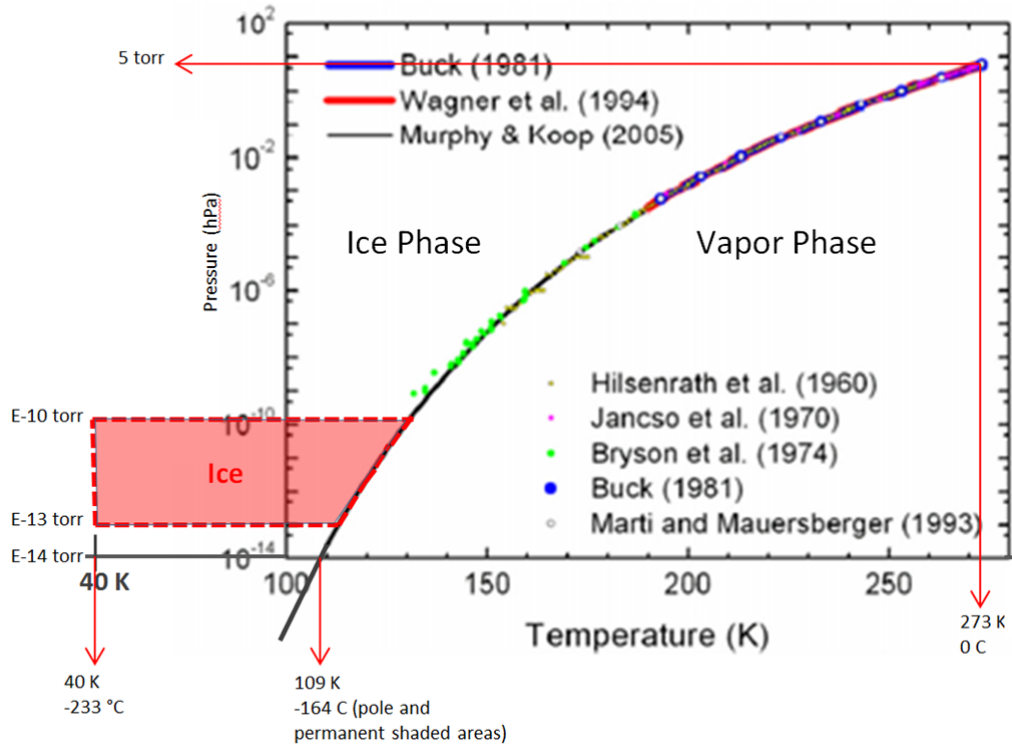


Figure 33. Ambient conditions on the Moon (colored in pink) that support the presence of water ice on the lunar surface

A.3 Mars Surface

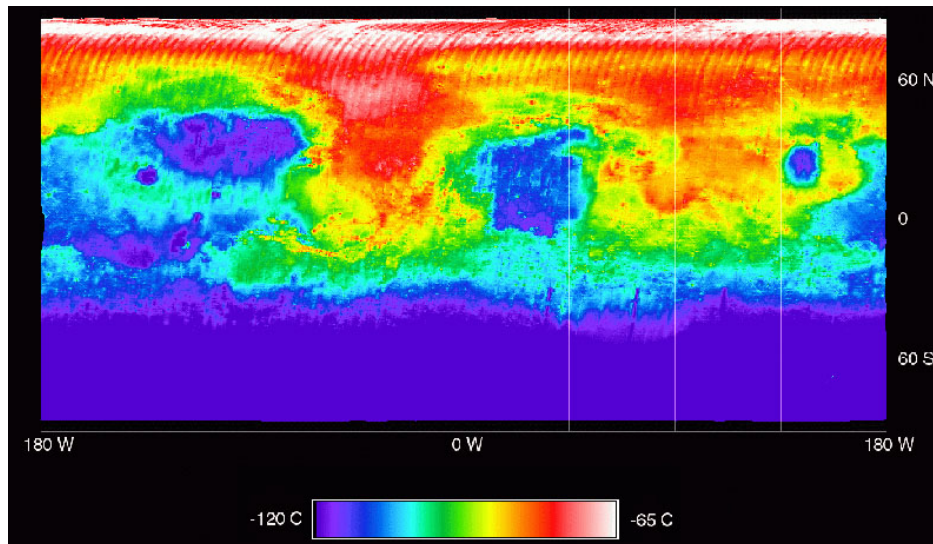


Figure 34. Mars surface temperature profile measured at night by the Thermal Emission Spectrometer (TES) onboard the Mars Global Surveyor spacecraft

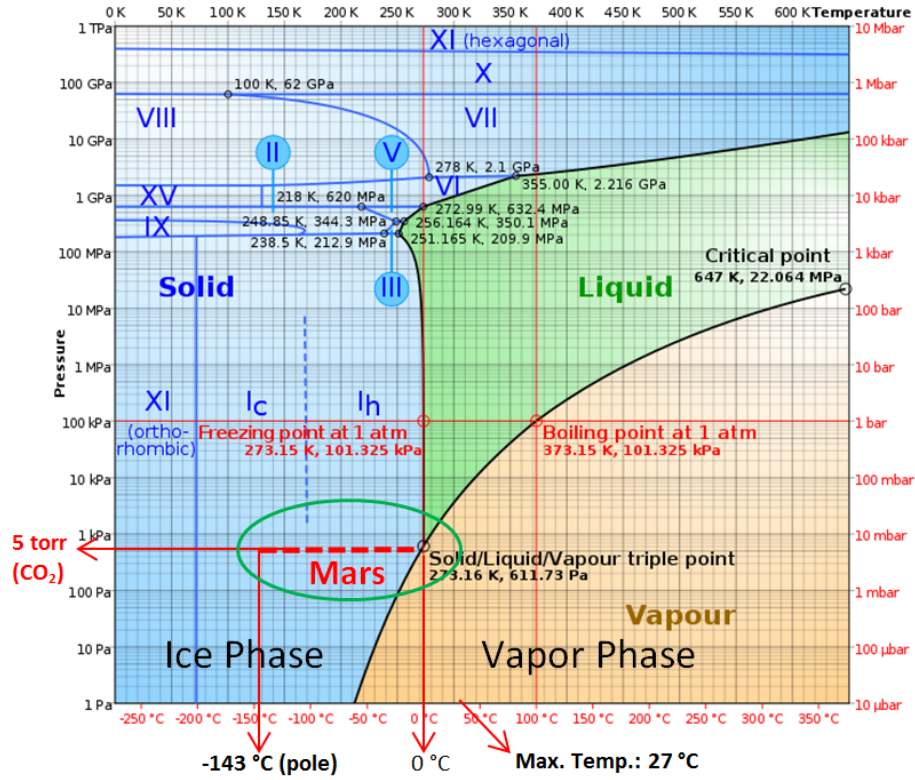


Figure 35. Ambient conditions on Mars (marked with dashed red line) that would support the presence of water ice on the Mars surface

A.4 Comet Surface

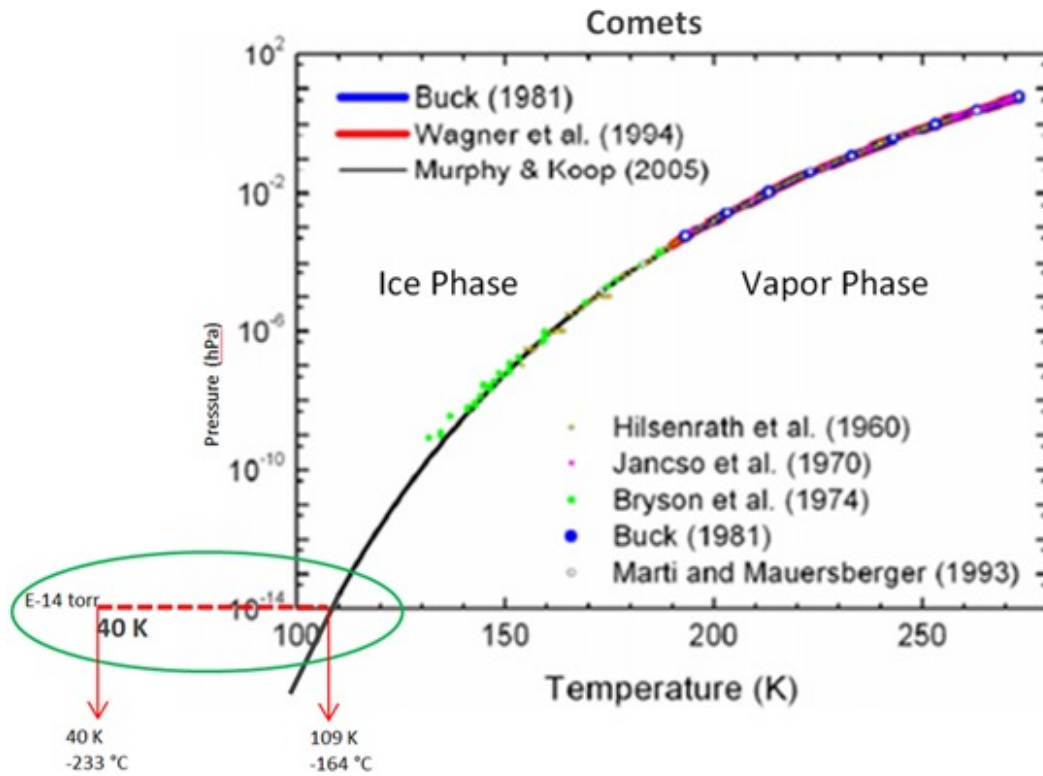


Figure 36. Ambient conditions on a comet (marked with dashed red line) that would support the presence of water ice on the comet's surface

A.5 Europa Surface

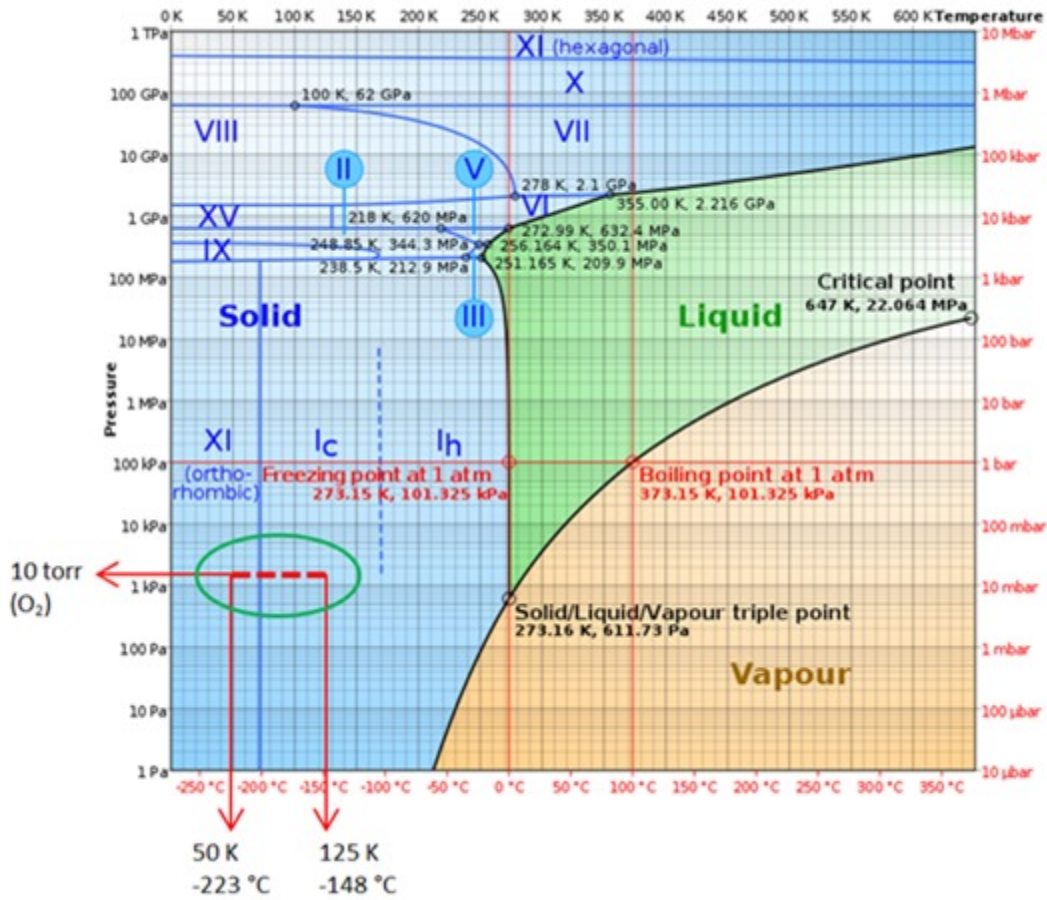


Figure 37. Ambient conditions on Europa (marked with dashed red line) that would support the presence of water ice on Europa’s surface

A.6 Titan Surface

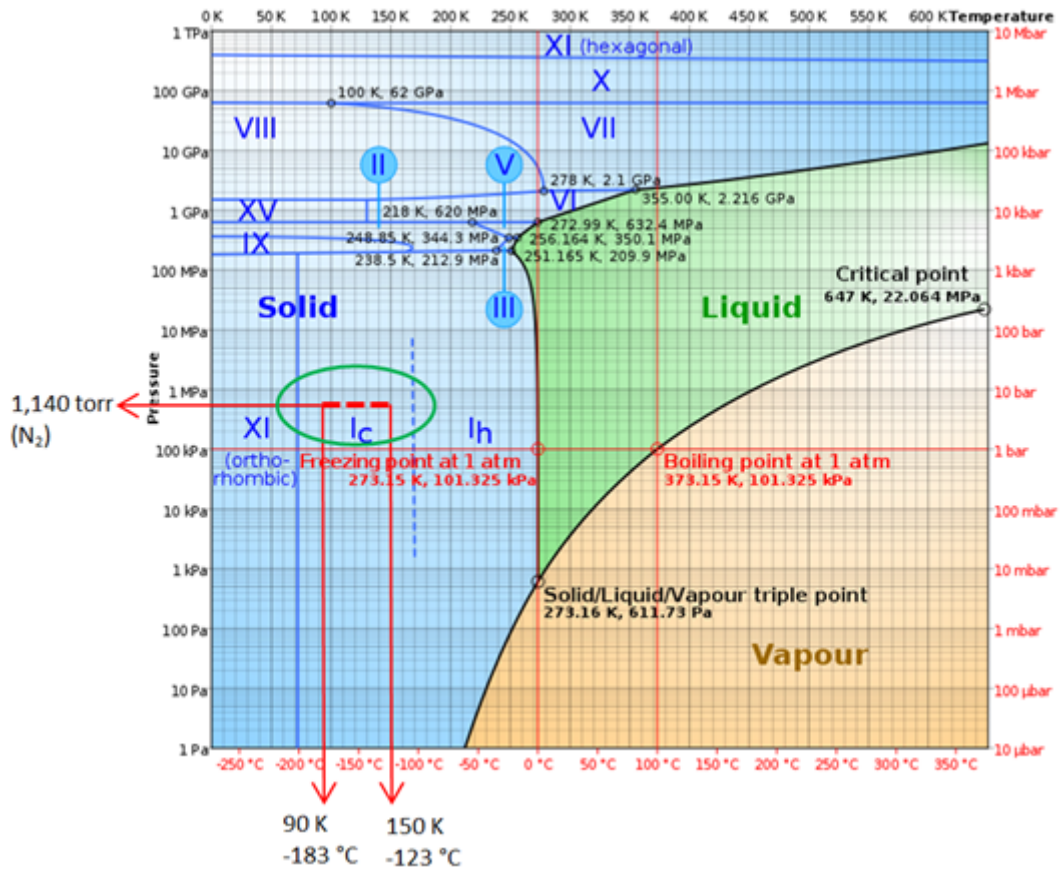


Figure 38. Ambient conditions on Titan (marked with dashed red line) that would support the presence of water ice on Titan’s surface

A.7 Appendix A References

- [1] http://en.wikipedia.org/wiki/Phase_diagram
- [2] Edgar L Andreas, *New estimates for the sublimation rate for ice on the Moon*, Volume 186, Issue 1, January 2007, page 26.

Appendix B. PHASE CONDITIONS OF CO₂ IN THE SOLAR SYSTEM

Conditions that Support the Presence of Ice CO₂ on the Surfaces of the Moon, Mars, Comets, Europa, and Titan

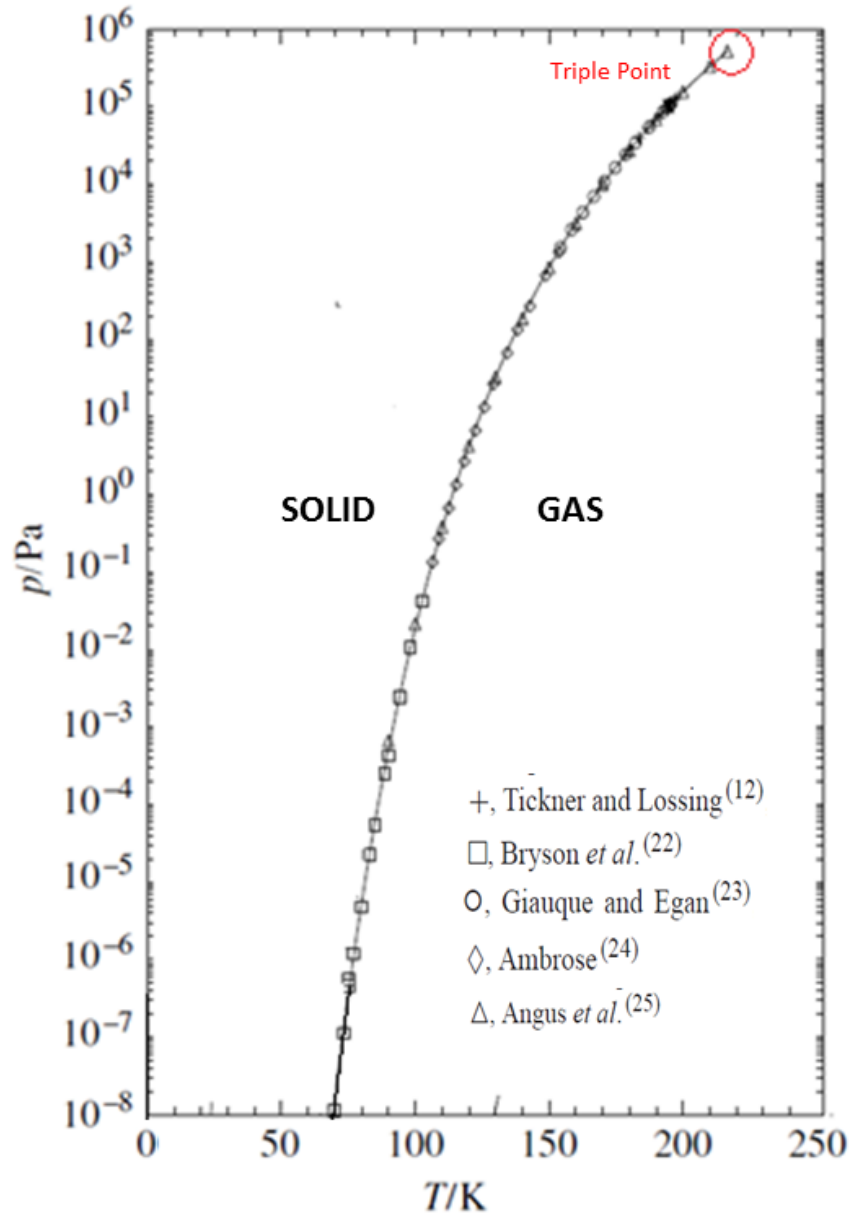


Figure 39. CO₂ solid-gas phase equilibrium estimated and reported independently by several authors [1]

B.1 CO₂ on Moon Surface

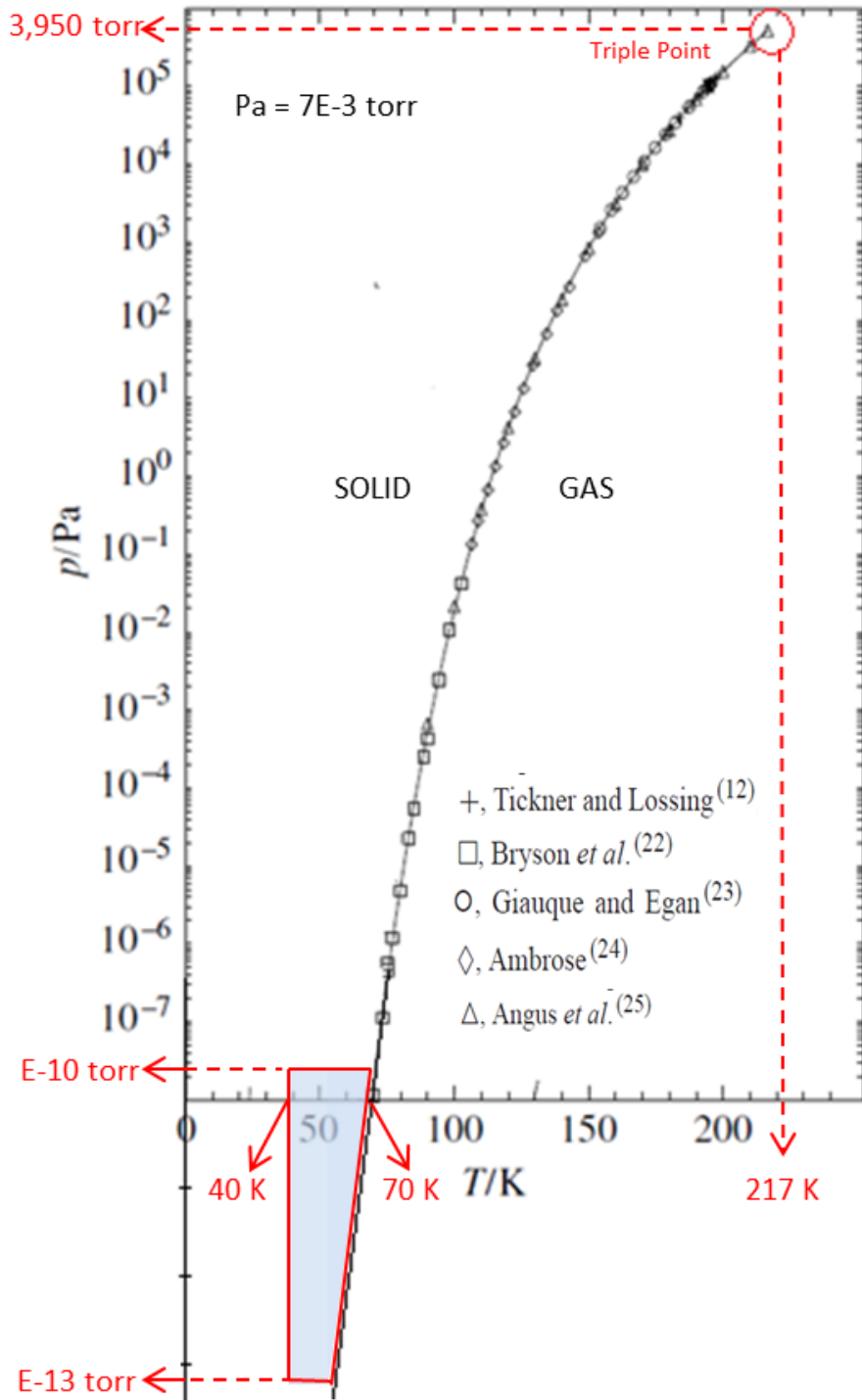


Figure 40. Ambient conditions on the Moon (colored in blue) that support the presence of CO₂ ice on the lunar surface

B.2 CO₂ Ice on Mars Surface

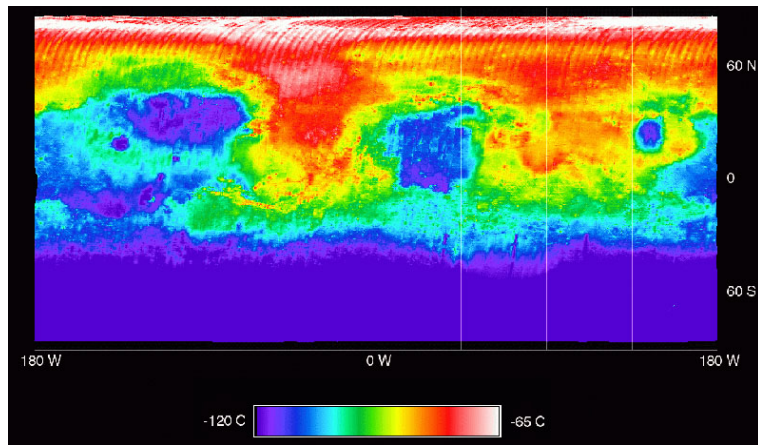


Figure 41. Mars surface temperature profile measured at night by TES onboard the Mars Global Surveyor spacecraft

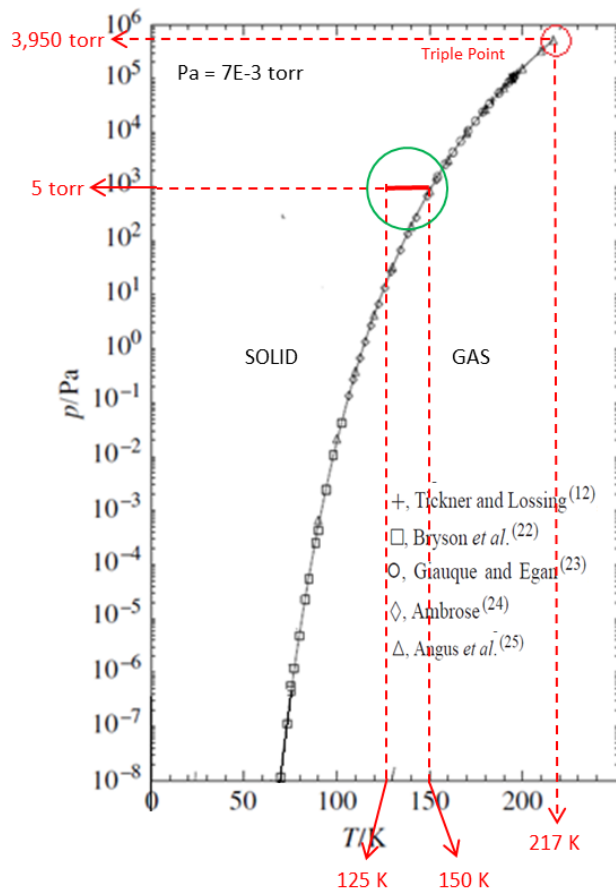


Figure 42. Ambient conditions on Mars (marked with continuous red line) that would support the presence of CO₂ ice on the Mars surface

B.3 CO₂ on Comet Surfaces

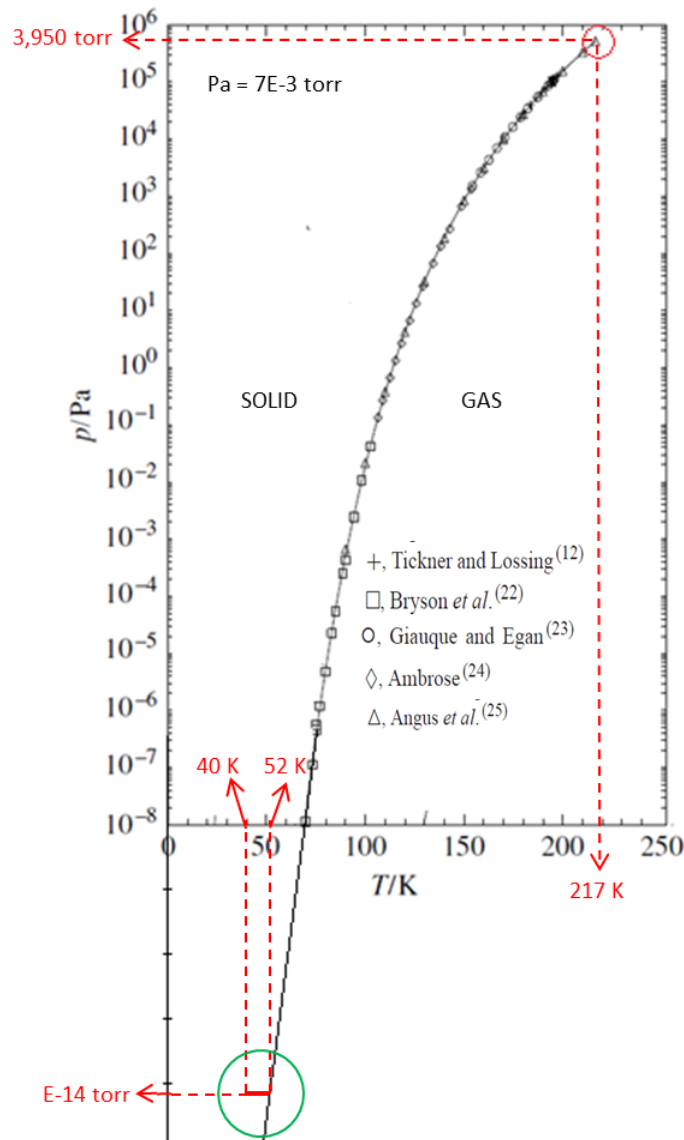


Figure 43. Ambient conditions on a comet (marked with continuous red line) that would support the presence of CO₂ ice on the comet's surface.

B.4 CO₂ on Europa

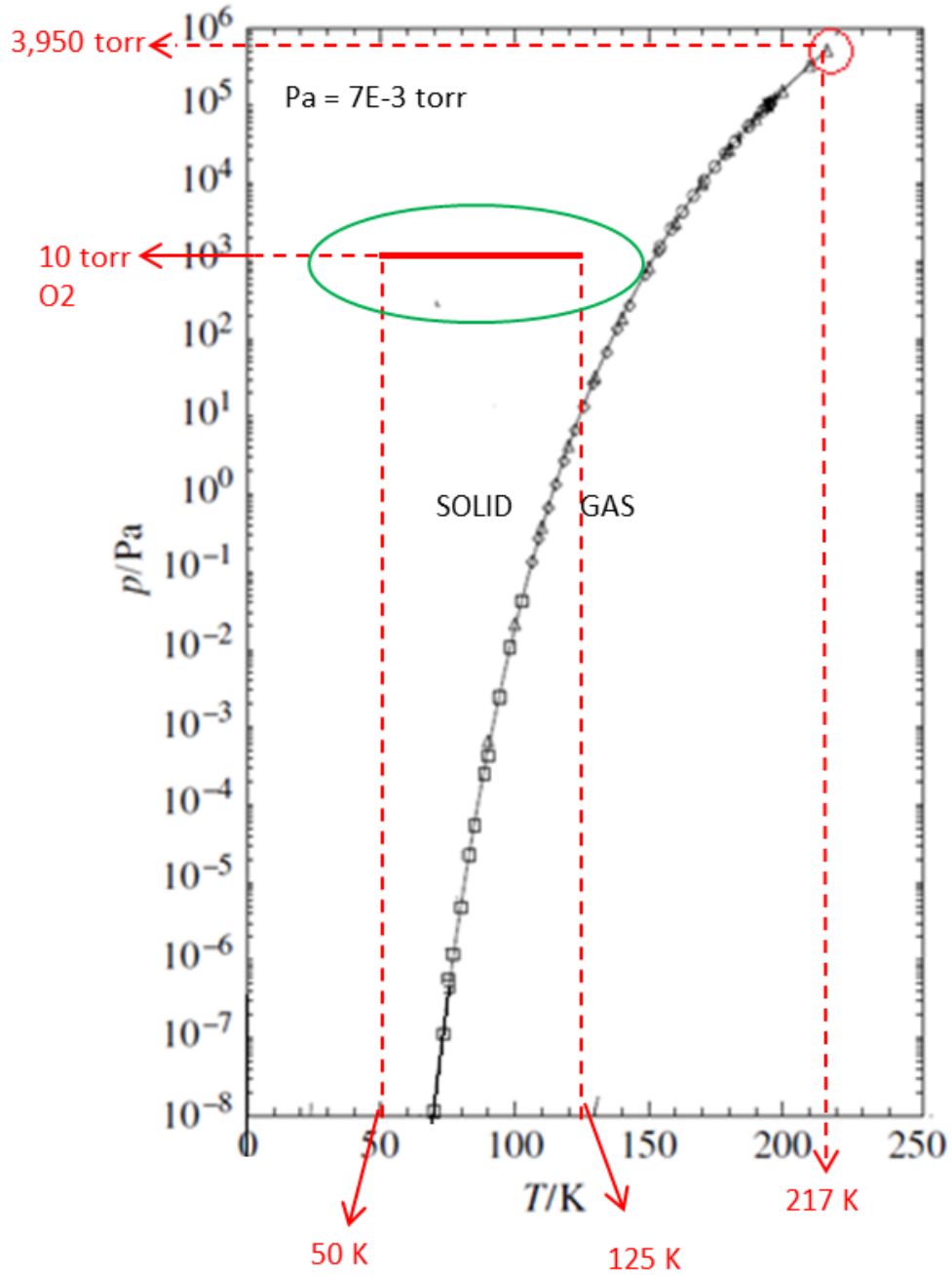


Figure 44. Ambient conditions on Europa (marked with continuous red line) that would support the presence of CO₂ ice on Europa's surface

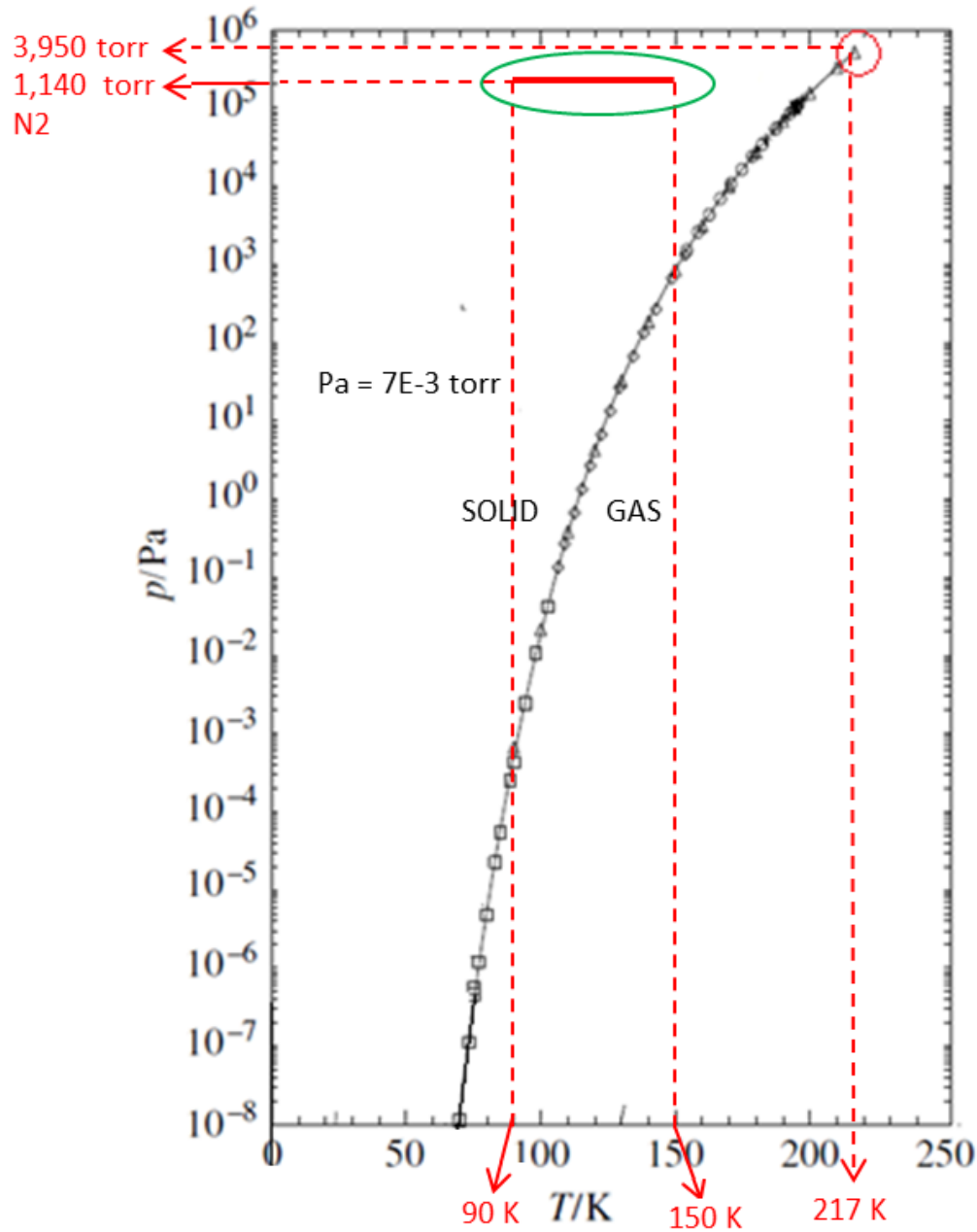
B.5 CO₂ on Titan Surface

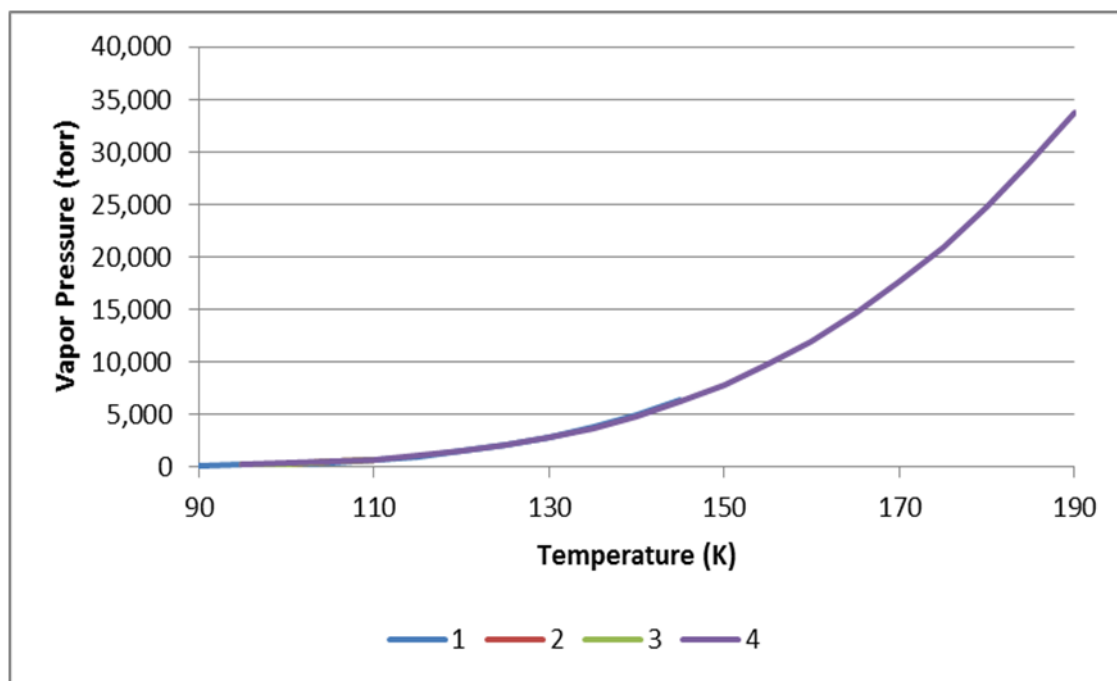
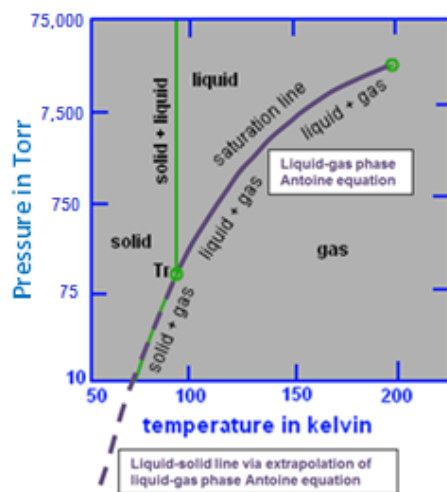
Figure 45. Ambient conditions on Titan (marked with continuous red line) that would support the presence of CO₂ ice on Titan's surface

B.6 Appendix B References

- [1] L'elio Q. Loba and Abel G. M. Ferreira, "Phase equilibria from the exactly integrated Clapeyron equation," *J. Chem. Thermodynamics* 2001, 33, page 1603.

Appendix C. **PHASE CONDITIONS OF CH₄ IN THE SOLAR SYSTEM**

**Conditions That Support the Presence of CH₄ Ice on the Surface of the Moon, Mars,
Comets, Europa, and Titan**

C.1 CH₄ Sublimation Phase

| | Temperature (K) | A | B | C | Reference | Comment |
|---|-----------------|---------|---------|---------|----------------------------|---|
| 1 | 90.99 - 189.99 | 3.9895 | 443.028 | -0.49 | Prydz and Goodwin, 1972 | Coefficients calculated by NIST from author's data. |
| 2 | 96.89 - 110.19 | 2.00253 | 125.819 | -48.823 | Regnier, 1972 | Coefficients calculated by NIST from author's data. |
| 3 | 93.04 - 107.84 | 3.80235 | 403.106 | -5.479 | Cutler and Morrison, 1965 | Coefficients calculated by NIST from author's data. |
| 4 | 110.00 - 190.5 | 4.22061 | 516.689 | 11.223 | Hestermans and White, 1961 | Coefficients calculated by NIST from author's data. |

Figure 46. CH₄ sublimation equilibrium measurement and estimation of Antoine parameters (A, B, & C) independently obtained by four authors within the temperature range of 91-190 K [1]. This liquid-gas saturation line is extrapolated (dashed line) to predict sublimation line at lower temperature and pressure

C.2 CH₄ on Moon Surface

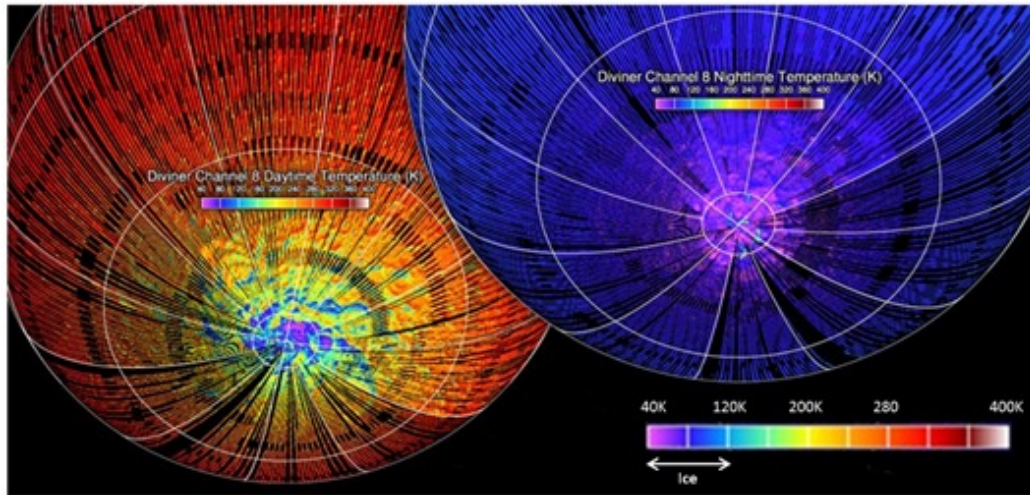


Figure 47. Daytime and nighttime temperature observations of the lunar south pole recorded by the Diviner Radiometer Experiment, one of seven instruments on NASA's Lunar Reconnaissance Orbiter

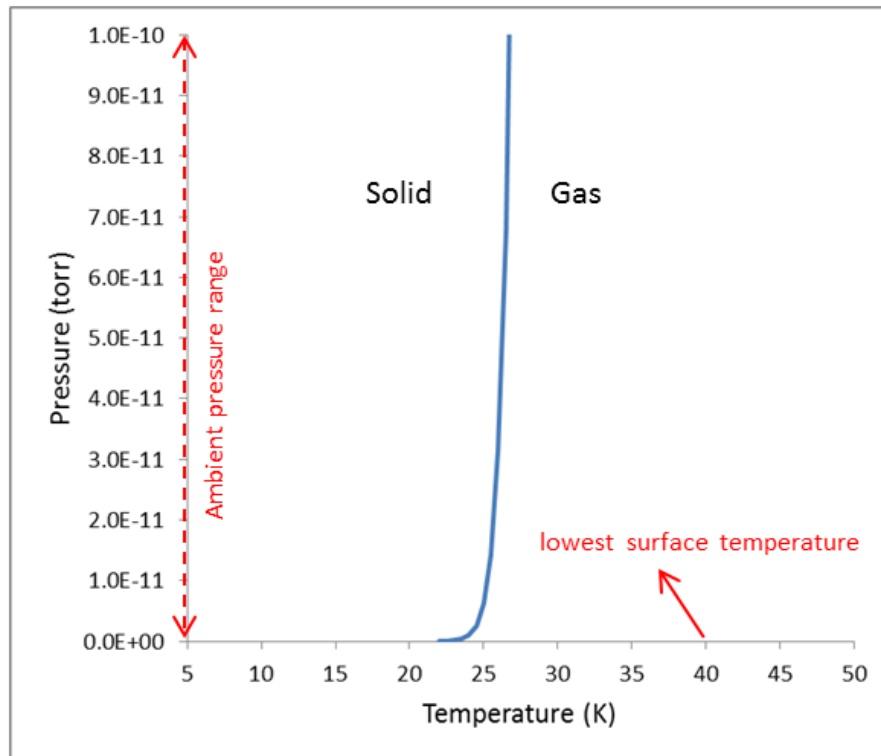


Figure 48. CH₄ ice is not likely to be present on the lunar surface because the Moon's lowest surface temperature of 40 K is higher than 25 K, the highest temperature at which CH₄ ice exists at the Moon's ambient pressure range (10^{-10} to 10^{-14} torr)

C.3 CH₄ Ice on Mars Surface

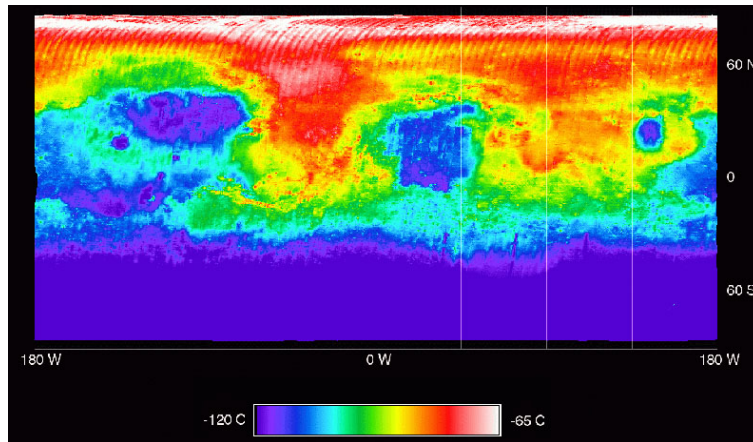


Figure 49. Mars surface temperature profile measured at night by TES onboard the Mars Global Surveyor spacecraft

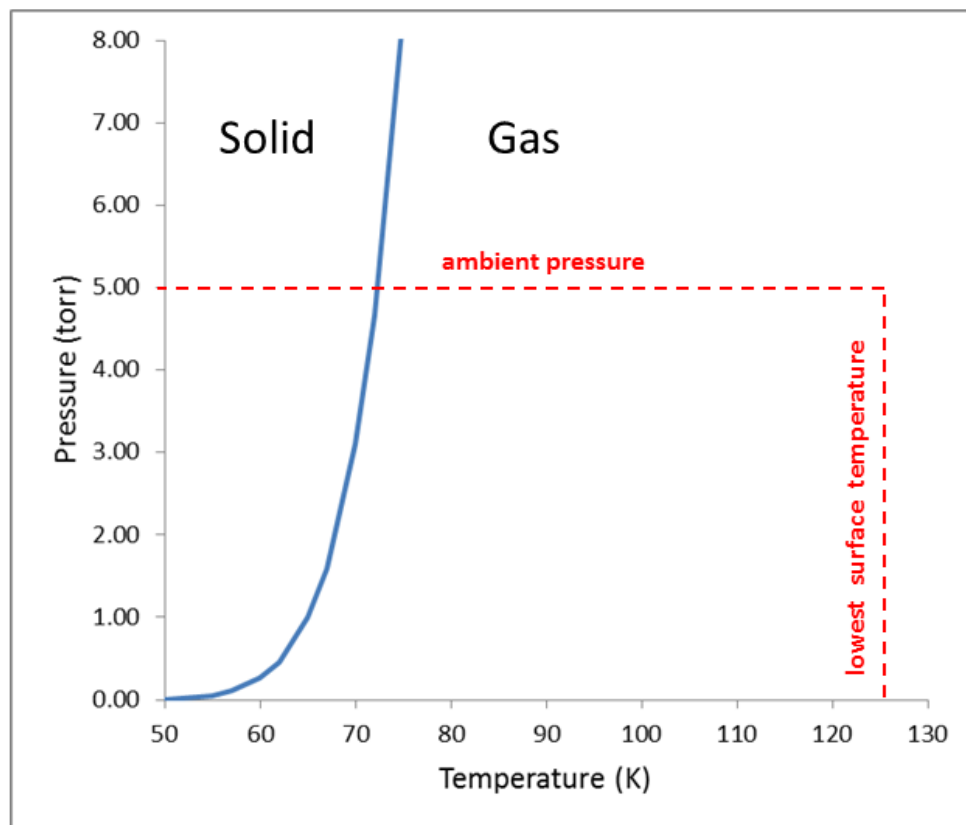


Figure 50. CH₄ ice is not likely to be present on the Mars surface because the lowest Mars surface temperature is 125 K and CH₄ vapor pressure at 125 K is 2,000 torr, much higher than the Mars ambient pressure (5 torr)

C.4 CH₄ on Comet Surfaces

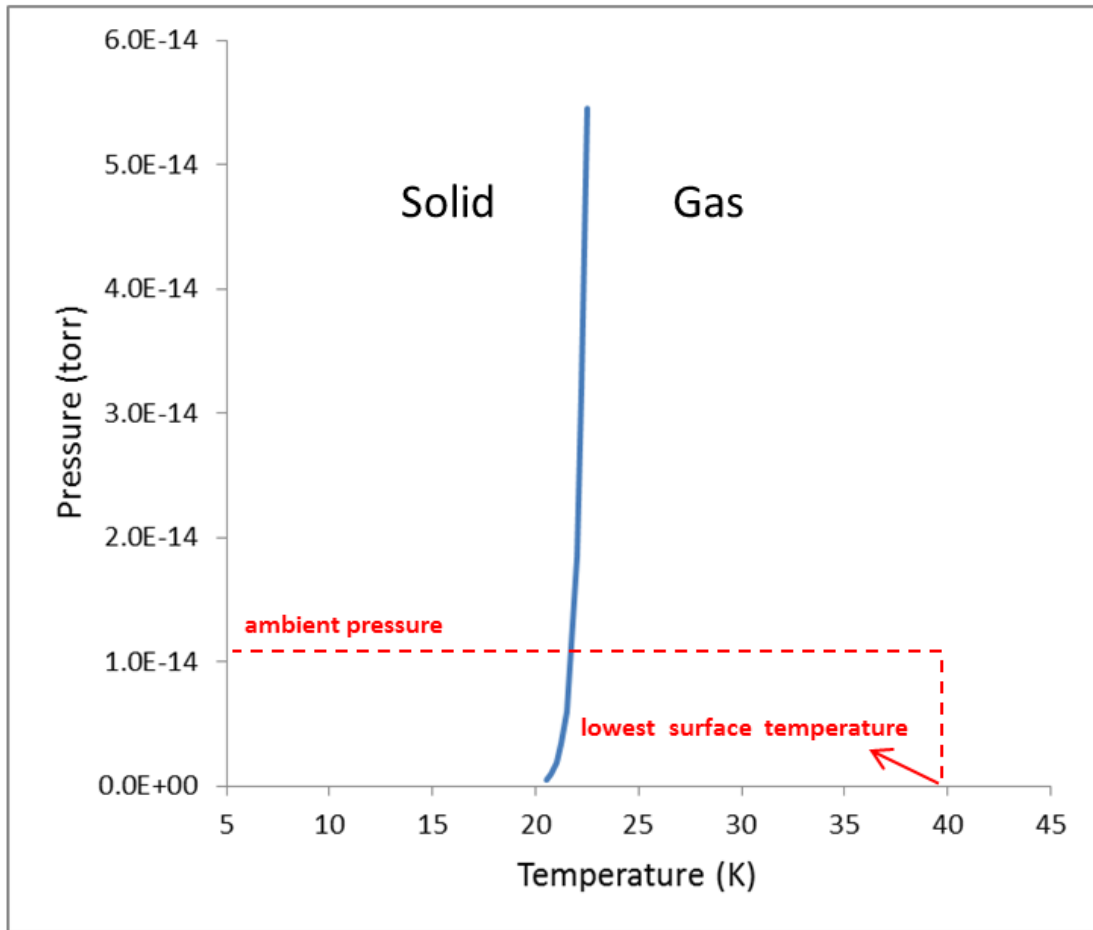


Figure 51. CH₄ ice is not likely to be present on a comet's surface because the lowest comet surface temperature 40 K is higher than 22 K, the highest temperature at which CH₄ ice exists at the comet's ambient pressure (10⁻¹⁴ torr)

C.5 CH₄ on Europa

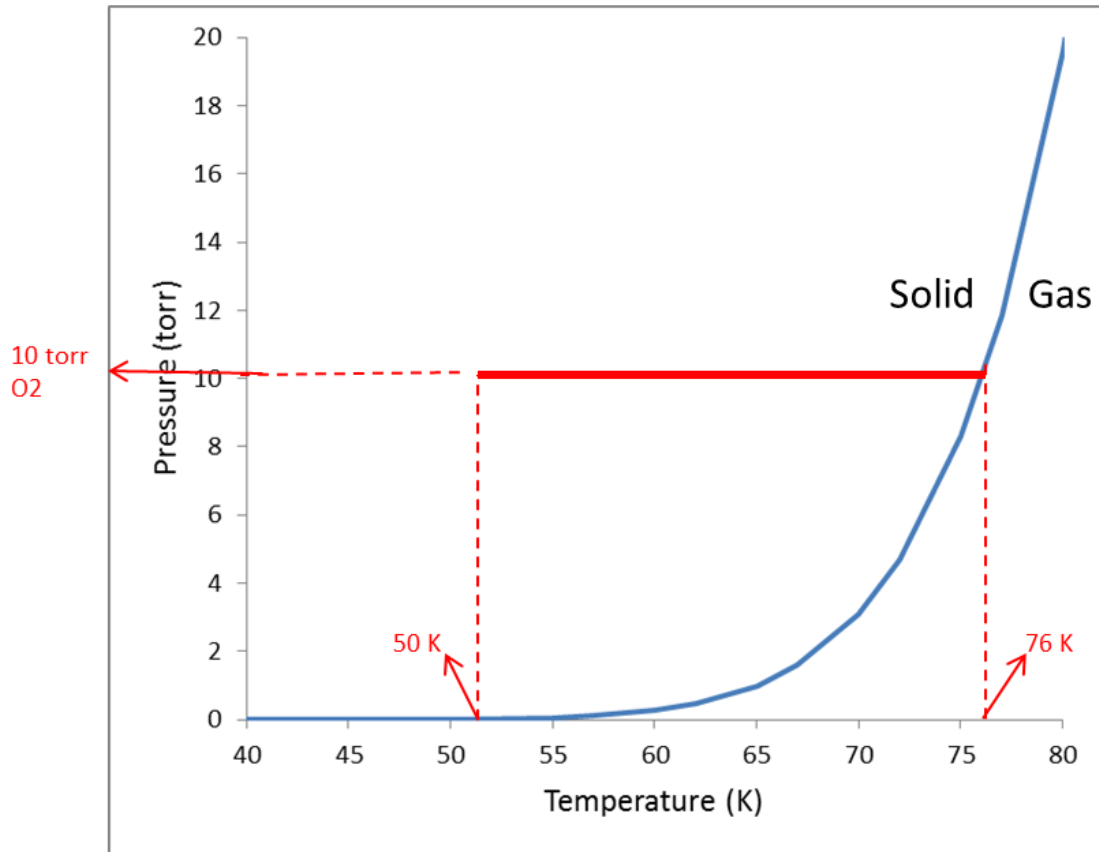


Figure 52. Ambient conditions on Europa (marked with continuous red line) that would support the presence of CH₄ ice on Europa's surface

C.6 CH₄ on Titan Surface

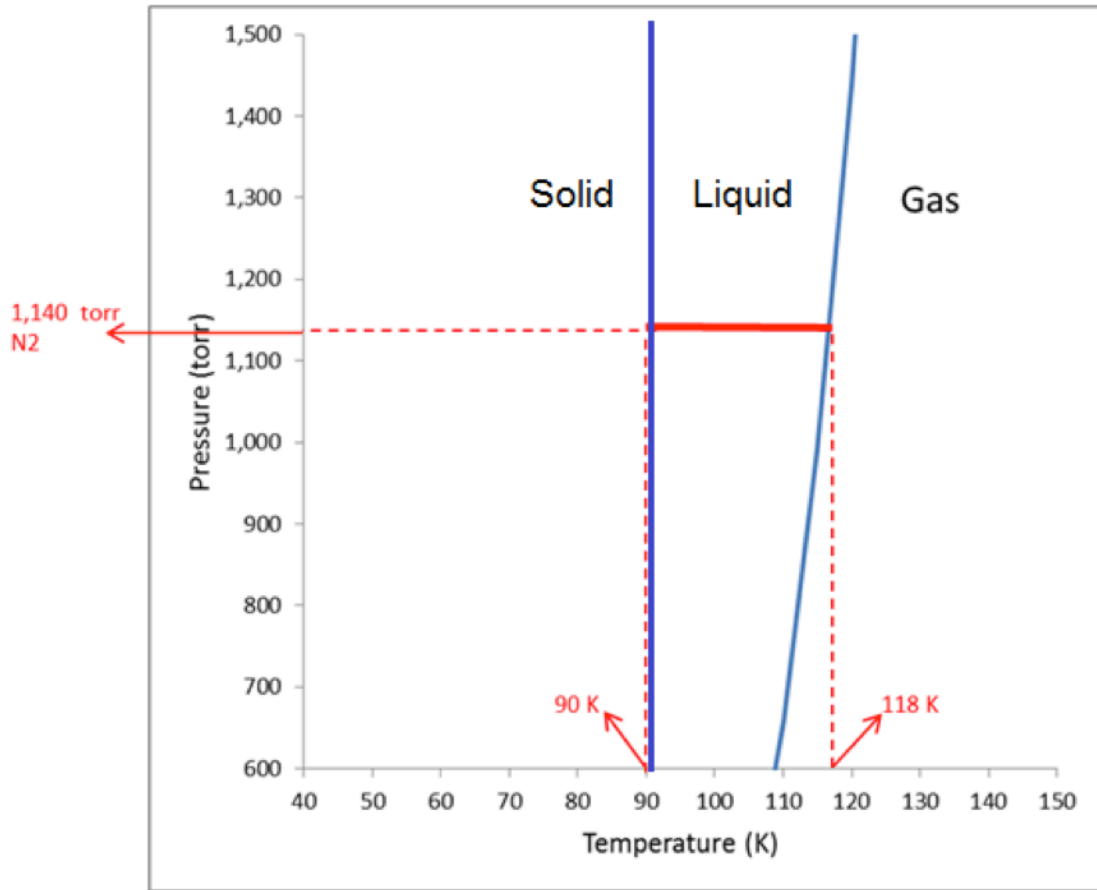


Figure 53. Ambient conditions on Titan (marked with continuous red line) that would support the presence of liquid CH₄ on Titan's surface

C.7 Appendix C References

- [1] <http://webbook.nist.gov/cgi/cbook.cgi?ID=C74828&Mask=4>